Preparation of (bio)polymer matrices for substance transfer and study of their release

Ing. Monika Muchová, Ph.D.

Tomas Bata University in Zlín

Tomas Bata University in Zlín
Faculty of Technology

Doctoral Thesis Summary

Preparation of (bio)polymer matrices for substance transfer and study of their release

Příprava (bio)polymerních matric pro přenos látek a studium jejich uvolňování

Author:	**Ing. Monika Muchová, Ph.D.**
Degree programme:	Chemistry and Materials Technology (P2808)
Degree course:	Technology of Macromolecular Compounds (2808V006)
Supervisor:	prof. Ing. *et* Ing. Ivo Kuřitka, Ph.D. *et* Ph.D.
Consultant:	Mgr. Jan Vícha, Ph.D.
Reviewers:	prof. Ing. Vladimír Sedlařík, Ph.D.
	doc. Ing. Lucy Vojtová, Ph.D.

Zlín, January 2024

ACKNOWLEDGEMENT

I would like to convey my sincere gratitude to my supervisor, Assoc. Prof. Ing. et Ing. Ivo Kuřitka, Ph.D. et Ph.D., for the continuous support during my doctoral study and research, imparting knowledge and sharing his expertise with me. I would also like to extend my thanks to my consultant Mgr. Jan Vícha, Ph.D. for his motivation, patience, widening of the knowledge, guidance, and encouragement. I would also like to thank Ing. Lukáš Münster, Ph.D., for help with experimental work and enrichment of knowledge.

I am grateful to my colleagues and friends at the Centre of Polymer Systems for their assistance, advice, and companionship during my studies.

My special thanks are devoted to Kateřina Štěpánková for being my soulmate and emotional support. I would like to thank Alžběta Důbravová for endless positivity and support throughout my research journey.

Special thanks belong to my family for all the support, patience, encouragement, strength, and never losing hope in me.

ABSTRACT

The thesis focuses on the study of hydrogel films prepared from the oxidized polysaccharide crosslinkers and polyvinyl alcohol (PVA) aimed at biomedical applications, particularly drug delivery. Initially, the role of the matrix (PVA) characteristics was studied in hydrogels crosslinked by 2,3-dialdehyde cellulose (DAC) and designed for the transdermal delivery of biologically active compounds. Hydrogel structure, properties, and drug release kinetics were investigated. Optimization was achieved by varying the amounts of DAC crosslinker and weight average molecular weight (M_w) of PVA. The best results were obtained for hydrogel films using 0.25% wt. DAC and PVA with M_w=130 kDa which had high porosity, drug loading capacity, mechanical properties, and skin adhesion among all tested samples. Next, different types of oxidized dialdehyde polysaccharide crosslinkers (DAP) based on cellulose, dextran, dextrin, and hyaluronic acid were compared on the selected PVA matrix, from which PVA/DAPs hydrogel films were created. The goal was to formulate a structure/function relationship and to select the best crosslinkers for a given application. The properties of PVA/DAP hydrogels were compared based on the density of -CHO groups, the structure of the crosslinkers, the molecular weight, and the size of the crosslinker nano-assemblies formed spontaneously in their solutions. All prepared hydrogel films with different amounts of DAC and M_w PVA crosslinker (PVA /DAC) and PVA/DAPs films were analyzed based on mechanical, viscoelastic properties, porosity, swelling, water content, network parameters, and cytotoxicity. Crosslinkers based on linear polysaccharides (cellulose, hyaluronate) performed more reliably, while the presence of branching could be both beneficial (dextran) and detrimental (dextrin) at lower crosslinker concentrations.

ABSTRAKT

Práce je zaměřena na studium hydrogelových filmů připravených z oxidovaných polysacharidových síťovacích činidel a polyvinylalkoholu (PVA) se zaměřením na biomedicínské aplikace, zejména podávání léčiv. Zpočátku byla studována role matrice (PVA) zesíťované 2,3-dialdehydcelulózou (DAC) v hydrogelech navržených pro transdermální podávání biologicky aktivních sloučenin. Byly zkoumány vlastnosti hydrogelu, struktura a kinetika uvolňování léčiva. Optimalizace bylo dosaženo změnou množství zesíťovacího činidla DAC a hmotnostní průměrné molekulové hmotnosti (M_w) PVA. Nejlepších výsledků bylo dosaženo u hydrogelových filmů s použitím 0,25 % hm. DAC a PVA s M_w=130 kDa, které měly vysokou poréznost, kapacitu nanášení léčiva, mechanické vlastnosti a adhezi ke kůži u všech testovaných vzorků. Dále byly porovnány různé typy oxidovaných dialdehydových polysacharidových síťovacích činidel (DAP) na bázi celulózy, dextranu, dextrinu a kyseliny hyaluronové na vybrané PVA matrici, ze které byly vytvořeny PVA/DAPs hydrogelové filmy. Cílem bylo formulovat vztah struktura/funkce a vybrat nejlepší síťovací činidla pro danou aplikaci. Vlastnosti PVA/DAP hydrogelů byly porovnány na základě hustoty -CHO skupin, struktury síťovacích činidel, molekulové hmotnosti a velikosti nano-souborů síťovacích činidel, které se spontánně vytvořily v jejich roztocích. Všechny připravené hydrogelové filmy s různým množstvím DAC a M_w PVA síťovadla (PVA/DAC) a PVA/DAPs filmy byly analyzovány na základě mechanických, viskoelastických vlastností, porozity, botnání, obsahu vody, síťových parametrů a cytotoxicity. Síťovací činidla na bázi lineárních polysacharidů (celulóza, hyaluronát) fungovala spolehlivěji, zatímco přítomnost větvení by mohla být prospěšná (dextran) i škodlivá (dextrin) při nižších koncentracích síťovacích činidel.

TABLE OF CONTENT

1. INTRODUCTION

Biopolymers are biodegradable materials made from renewable sources by living organisms[1,2]. The repeating units of saccharides, nucleic acids, or amino acids form the backbone of their molecules, and sometimes, side chains also contribute to their functions. Some natural polymers such as polysaccharides provide energy for cell activity and function as structural components in living systems, other polymers produced by microorganisms, plants or animals manipulate basic biological information such as proteins and nucleic acids. In addition to their importance in biology, materials such as chitin, collagen, cellulose, or starch have over time proven their use for various applications in packaging, food, textile, medical, agricultural, and other industries[1]. Utilization of biopolymers has increased significantly across almost all aspects of life as a result of the ongoing health and environmental issues of synthetic polymers.

Hydrogel-based biomaterials are receiving ever-increasing attention due to their similarity to living tissues in terms of mechanical properties, porosity, and high water content. Due to their ability to capture, store, and release substances, hydrogels are excellent materials for various drug delivery applications as well as wound dressings[3–5].

An important aspect of the use of hydrogels in pharmacy is their low toxicity, biocompatibility, and suitable mechanical properties. While synthetic polymer-based hydrogels have well-defined structures and properties, they have also drawbacks. For instance, fully synthetic hydrogels, such as PVA hydrogels crosslinked with organic dialdehydes like glutaraldehyde[6], have a relatively high level of toxicity due to the use of low molecular weight cross-linking compounds. On the other hand, purely biopolymer-based hydrogels have better biodegradability, but in the swollen state, they often have poor mechanical properties. One possible answer is the use of hybrid hydrogels made from two polymers of natural and synthetic origin[7]. These have better-defined properties and can be optimized more easily[3–5]. Polysaccharides such as cellulose, hyaluronan, dextran, and dextrin are potential candidates as they can be obtained from renewable sources, contain vicinal diols in their structure, and can be selectively oxidized to aldehyde groups to prepare dialdehyde polysaccharides (DAPs) [8–10], which are perfect for crosslinking matrices rich in hydroxyl groups, like PVA[11]. Here we investigate the synthesis, properties, and applications of DAP/PVA hydrogels.

2. HYDROGELS

Hydrogels are three-dimensional cross-linked structures that can absorb large amounts of water based on their hydrophilic nature [12–14]. Their hydrophilicity arises from the presence of hydrophilic groups such as -OH, -COOH, -CONH$_2$, -CONH-, -SO$_3$H etc. They can also have a main chain made of a water-soluble polymer, such as derivatives of poly(ethylene oxide), or can be based on ionomers, glycopolymers, acrylic, acrylamide, N-vinyl-2-pyrrolidinone, or poly(vinyl alcohol)[13].

2.1 Characterization and structure

The structure of the hydrogel network is determined by the presence of polymer chains that are covalently or physically linked into a 3D arrangement. Polymer chains can be formed from a homopolymer or copolymer and those can form a single connected 3D network or an interpenetrating polymer network, i.e. two or more networks that are physically entangled with each other but not connected by covalent bonds[12]. Based on the structure of the polymer network, its interaction with the solvent, and the type of polymer, the properties of the hydrogel are given. For example, crosslinks between different polymer chains result in different viscoelastic behavior and give the gel its structure and elasticity[15,16]. The properties of crosslinkers are thus paramount in designing hydrogels for given applications. Among the most important properties of a hydrogel is its ability to bind water, which depends on the density of the hydrogel network and the content of the hydrophilic monomer. Important parameters that ensure water absorption are the compatibility between the polyelectrolyte and water and the osmotic pressure created by the high concentration of ionic groups in the gel [15].

The structure of the hydrogel network is characterized by the volume fraction in the swollen state (v_2,s), which indicates the percentage of the gel matrix in the gel volume, the number-average molecular weight of the polymer chains between the crosslinks (M_c), and the network mesh size (ξ) which describes the distance between individual chains and allows the diffusional movement of solute molecules. By obtaining and comparing these parameters for a given type of hydrogel, it can be shown how effective a given crosslinker is. [12,17].

2.2 Release of substances from hydrogel systems

The permeability of substances that are not bound to the hydrogel network through an equilibrium swelled-state hydrogel is based on diffusion. Several criteria influence the diffusion behavior of these substances. One of them is the mesh size, which depends both on the concentrations of the polymer and the crosslinker, as well as on the external effects of temperature and pH. Due to network heterogeneity and polymer polydispersity, most hydrogels have a wide mesh size distribution [12,18]. Mesh size can be calculated based on the established

shear or Young's modulus or degree of swelling [19,20]. The hydrogel mesh size can also be obtained using the Flory-Rehner equilibrium swelling theory [21,22]. The classical theory of rubber elasticity relates the shear modulus G to the mesh size r $_{mesh}$ by [18]:

$$r_{mesh} = (\frac{6RT}{\pi N_{AV} G})^{1/3} \tag{1}$$

where R is the gas constant, T is the absolute temperature, and N_{AV} is Avogadro´s number.

To directly characterize the mesh size, techniques such as confocal microscopy, electron microscopy, atomic force microscopy, small-angle X-ray scattering (SAXS), and small-angle neutron scattering (SANS)[18,23,24] exist.

The size of the mesh determines the method of drug diffusion. If the mesh size is significantly larger than the drug, diffusion is mostly unhindered, and small drug molecules freely migrate through the network. By increasing the polymer or crosslinker concentrations, the mesh size can be decreased. As the drug size approaches the mesh size, its release begins to slow down considerably. If the mesh size is smaller than the drug, the drugs remain trapped inside the mesh. To release drugs, network degradation, swelling, or network deformation is required[18].

The empirical Korsmeyer-Peppas equation is utilized to describe the kinetics of substance release from hydrogel systems[18,25–27]:

$$\frac{M_t}{M_\infty} = kt^n \tag{2}$$

where M_t is the mass of the drug released at time t, M_∞ is the total mass of the drug released, k is the kinetic constant, and n is the diffusion exponent. The size of the exponent n depends on the type of transport, the shape of the hydrogel, and the polydispersity of the polymer. If n=0.5, the drug is released by Fickian diffusion. If n=1 surface erosion dominates. In general, real systems often have n between 0.5 and 1 because more than one mechanism controls release in a given system.

3.   DIALDEHYDE POLYSACCHARIDES

Polysaccharides are formed of monosaccharide units that are linked by glycosidic bonds. Polysaccharides are very abundant in nature and are easily derived from various natural sources. Thus, they offer a wide development potential due to their excellent properties, which include natural abundance, biocompatibility, biodegradability, chemical reactivity, etc[28]. Due to the existence of various functional groups in the structure of polysaccharides, the chemical properties of polysaccharides can be changed by chemical modifications. In particular, polysaccharides containing vicinal diol(s) can be selectively oxidized to introduce aldehyde groups to prepare dialdehyde polysaccharides[10,28].

3.1 Preparation, structure and properties

Dialdehyde polysaccharides (DAPs) are generally prepared by regioselective oxidation of source polysaccharides that contain neighboring (vicinal) -OH groups using periodate salt, which introduces a pair of reactive aldehyde groups into each oxidized unit [29,30]. This reaction is shown in Figure 1[31].
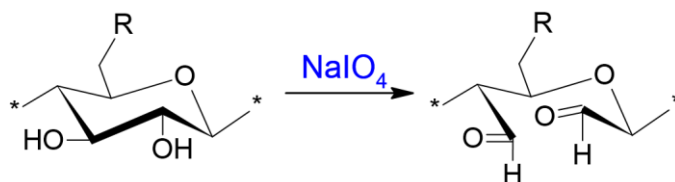

Figure 1 Periodate oxidation of polysaccharide featuring vicinal diol group at C2 and C3[31]

The structures of DAPs are closely linked to the architecture of source polysaccharides. The structures of source polysaccharides used in this work and respective dialdehydes are given in Figure 2 [31].

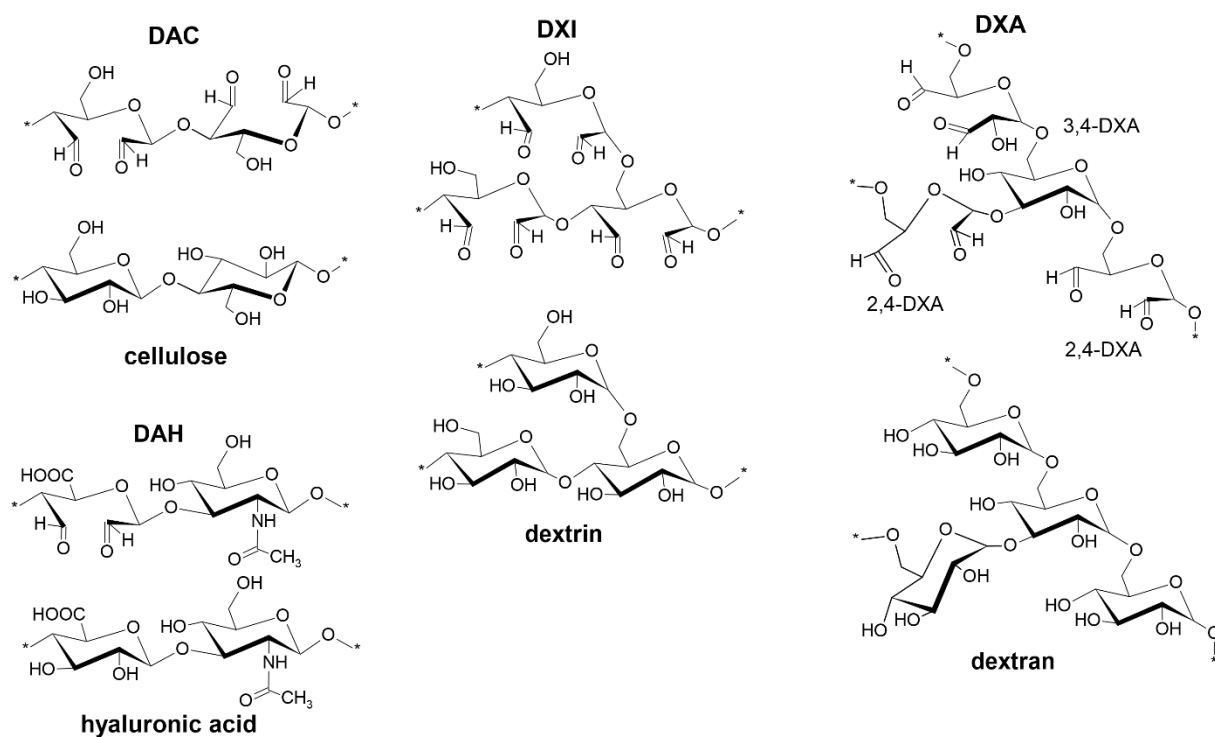*Figure 2: Structures of source polysaccharides and corresponding dialdehydes[31]*

Cellulose is one of the most abundant polysaccharides worldwide and can be found in various plants, tunicates, and bacteria. It is composed of linear chains of anhydroglucose units (AGU) linked by β-(1→4) glycosidic bonds. The oxidation of cellulose by periodate is characterized by cleavage of the C2–C3 bond of AGU,

leading to the formation of 2,3-dialdehyde cellulose (DAC) [30]. It is thus highly regioselective.

Dextrin is a product of the hydrolysis of starch or glycogen. Due to the presence of α-(1→4) and α-(1→6) glycosidic bonds, dextrin forms a branched structure, see Figure 2. Depending on its molecular weight, it is partially or fully soluble in water. Oxidation of dextrin with periodate produces 2,3-dialdehyde dextrin (DXI) in a way analogous to DAC.

Complex glucans called dextrans are produced by microorganisms, particularly bacteria from the species *Leuconostoc* and *Streptococcus*. They are composed of AGU chains linked mainly by α-(1→6) glycosidic bonds with a degree of α-(1→3) branching. The structure and properties of dextran differ not only for different species of bacteria but also for different strains [32]. Because α-(1→6) bonded units contain three neighboring -OH groups, oxidation of dextran leads to a mixture of 3,4-, 2,4- and 2,3 dialdehyde dextrans (DXA) [33,34]. In contrast, AGUs with α (1→3) branching lack any vicinal hydroxyl groups and are therefore entirely resistant to periodate oxidation [29].

D-glucuronic acid and N-acetyl-D-glucosamine connected by alternating β-(1→4) and β-(1→3) glycosidic links form the anionic linear polysaccharide known as hyaluronic acid (HA). Compared to cellulose, only the D-glucuronic acid units contain vicinal diols and are oxidized, because the glycosidic link at position C3 protects the N-acetyl-D-glucosamine units from periodate oxidation, see Figure 2. This reduces the maximum amount of -CHO groups per unit of HA mass to 5 mmol/g, i.e. by a factor of 2.5 compared to cellulose/DAC (12.5 mmol/g). HA is abundant in the human extracellular matrix, synovial fluid, cartilage, muscle connective tissue tissues, skin, etc. [35,36]

3.2 Applications

Based on the presence of reactive aldehyde groups, DAPs are used for different purposes. For instance, DAC is used as a filling for cellulose-based columns in aqueous chromatography[37], an absorbent of heavy metal ions and dyes[38], a material for protein immobilization[39], a carrier for drug delivery[40], material in tissue engineering[41], and has applications in wound dressings[31]. DAH has been used, for example, as a crosslinker for hydrogels intended for chronic wound treatment and tissue regeneration[42,43]. Oxidized dextran is used for wound healing as a cross-linking agent for polymers containing amine groups, such as chitosan[44]. Applications of dextrin derivatives are mostly limited to cyclodextrins, which are used as carriers for hydrophobic types of drugs[45], improving the ability of hydrogels to load drugs and control their release[46].

This work focuses on oxidized cellulose, dextran, dextrin, and hyaluronic acid and their use as crosslinkers for PVA.

4. POLY(VINYL ALCOHOL) BASED HYDROGELS

Poly(vinyl alcohol) (PVA) is a linear semi-crystalline polymer that consists of a main carbon chain containing hydroxyl (-OH) functional groups. It is obtained by hydrolysis of polyvinyl acetate (PVAc). By controlling the hydrolysis step, different degrees of hydrolysis (DH) of the PVA polymer can be prepared, which thereby affects the behavior of the polymer such as solubility, crystallinity, and chemical properties[47,48].

Poly(vinyl alcohol) is one of the most widespread and used materials for hydrogel applications, due to its biocompatibility, biodegradability, low toxicity, etc.[49,50] Based on these properties, PVA can be used for various purposes such as the formation of films, hydrogels, fibers, scaffolds, composites, or polymer membranes[47]. Hydrogels can be prepared from PVA by cross-linking hydroxyl groups to form hydrogels[51].

4.1 Preparation of PVA-based hydrogels

PVA-based hydrogels can be prepared in different ways that determine their network parameters and physico-chemical properties.

The first method is physical cross-linking using freeze-thaw-induced crystallization or high-temperature (energy) processing, where network nodes are formed through prolonged heating.[52] The advantage is the absence of a cross-linking agent. On the other hand, partial degradation of PVA caused by higher temperatures can lead to the polymer degradation[53,54].

The second method is chemical crosslinking, using agents such as epichlorohydrin, various aldehydes (formaldehyde, glutaraldehyde, benzaldehyde, etc.), anhydrides (EDTA dianhydride) or boric acid[55,56]. A common feature of crosslinking agents is their synthetic origin (except boric acid) and relatively high toxicity. Therefore, an important step in the preparation of synthetic hydrogels is their intensive purification and removal of all potentially toxic reactive components that may be trapped in the gel network[54].

4.2 Applications

There are countless specific applications of cross-linked PVA hydrogels in many different fields due to the improvement of the physical and mechanical properties of PVA by the presence of other synthetic polymers or biopolymers[57]. For example, there are PVA-based double network hydrogels that serve as absorbers of heavy metal ions in waste-water treatment[58] or PVA-based membranes that are used in various separation processes[59,60]. A lot of attention is focused especially on the field of biomedicine, including tissue engineering[48], wound dressing applications[7], contact lenses, orthopedics[61], etc.[52,62–65]

5. AIM OF DOCTORAL THESIS

This work deals with the study of the preparation of hydrogels based on modified polysaccharides as crosslinkers for transdermal/systemic administration of biologically active substances, and the study of the influence of their properties and structure on the kinetics of drug release.

The aim is to investigate the impact of the PVA matrix on the prepared hydrogels and to optimize their properties for transdermal delivery of substances. Additionally, the research aims to examine the influence of crosslinking agent structures on the properties of the hydrogels.

A synthetic polymer matrix (PVA) and modified polysaccharides as crosslinkers were chosen for hydrogel preparation. These polysaccharides are regioselective oxidized to the appropriate aldehydes capable of cross-linking the selected matrice. First, dialdehyde cellulose (DAC) was found effective for cross-linking PVA matrices resulting in hydrogels with potential application for transdermal delivery of substances. Then, four different dialdehyde polysaccharides (DAP) crosslinker types based on cellulose, dextran, dextrin, and hyaluronic acid were selected to obtain deeper insight in the principles generally governing cross-ling of PVA matrices by the modified polysaccharides. The main research directions of the thesis can be divided into two objectives:

1. Preparation and study of the PVA/DAC hydrogels to evaluate the effects of the cross-linking agent concentration and used PVA polymer on the resulting hydrogel properties. The loading of selected model bioactive substances into prepared materials and determination of the kinetics of substance release.

2. Analysis and study of the influence of the PVA matrix and different crosslinker properties and structure on the characteristics of hydrogels, namely their mechanical and viscoelastic properties, porosity, swelling, water content, and network parameters.

6. EXPERIMENTAL PART

6.1 Materials

For the matrix evaluation study, hydrogels were prepared using poly(vinyl alcohol) (PVA) with 88% degree of hydrolysis and different M_w (130 and 31 kDa, respectively, Sigma Aldrich Co.). Alpha cellulose (M_w = 109 kDa) (Sigma Aldrich Co.) oxidized by sodium periodate ($NaIO_4$) (Penta, Czech Republic) to 2,3-dialdehyde cellulose (DAC) served as a crosslinker. Following source polysaccharides were employed in the study of the role of crosslinker structure PVA/DAPs hydrogels: cellulose SigmaCell type 20 (weight-average molecular weight M_w = 76 kDa, degree of polymerization DP = 468, polydispersity index PDI = 4.7; Sigma Aldrich Co.), dextran from Leuconostoc spp. (M_w = 71, DP = 449, PDI = 1.9; Sigma Aldrich Co.), dextrin from corn starch type I (M_w = 52 kDa, DP = 325, PDI = 2.3; Sigma Aldrich Co.), and sodium hyaluronate (M_w = 1.5 MDa, DP = 3740, PDI = 4.3; Contipro Ltd., Czech Republic). Poly(vinyl alcohol) PVA with 88% degree of hydrolysis (M_w=130 kDa) served as a matrix. Other chemicals involved in modifications and characterizations can be found in relevant papers.[31,66] All chemicals were of analytical purity and were used as received without further purification. Throughout the experiments, demineralized water with a conductivity of less than 0.1 µS/cm was used.

6.2 Sample preparations

Dialdehydes polysaccharides (DAPs)

The general procedure for preparing DAP is as follows. Individual DAPs, namely cellulose, hyaluronate, dextrin, and dextran, were oxidized with $NaIO_4$ according to earlier works [54,67,68] into their respective 2,3-dialdehyde derivatives (DAC, DAH, DXI, and DXA). The reaction mixtures were left to stir in the dark for different time intervals depending on the type of polysaccharide used. Specifically, DAC was stirred for 72 hours, DAH for 24 hours, DXI for 8 hours, and DXA for 4 hours, all at a temperature of 30 °C. Reactions were stopped by the addition of ethylene glycol. For the PVA/DAC hydrogels for transdermal drug delivery, the raw DAC was washed, filtered, suspended in water, solubilized at 80 °C for 7 hours, and cooled before being centrifuged for 10 minutes. The rest of the dialdehyde polysaccharides for use as the role of crosslinker structure in PVA hydrogels, like DAC was centrifuged and homogenized. DXI, which was partially soluble, was dialyzed for a day against demineralized water. The DAC suspension and DXI sample were then solubilized in an oil bath under reflux, at 80 °C for 2 hours. The resulting solutions were purified by filtering and centrifugation to eliminate any residual insoluble material. Subsequently, they were dialyzed again for a day using 14 kDa MWCO dialysis tubing. All of the purified materials were then frozen using an ethanol ice bath and lyophilized,

resulting in dialdehyde polysaccharide powders (DAPs). The dialdehyde polysaccharide powders were utilized as crosslinkers for different PVA matrices.

Hydrogel preparation

The hydrogels are formed through a reaction between the crosslinker and the matrix involving the -CHO and -OH groups of the dialdehydes and PVA in an acidic environment. The dialdehyde polysaccharides (DAP) react with the hydroxyl groups of PVA to form hemiacetal bonds (Figure 3).
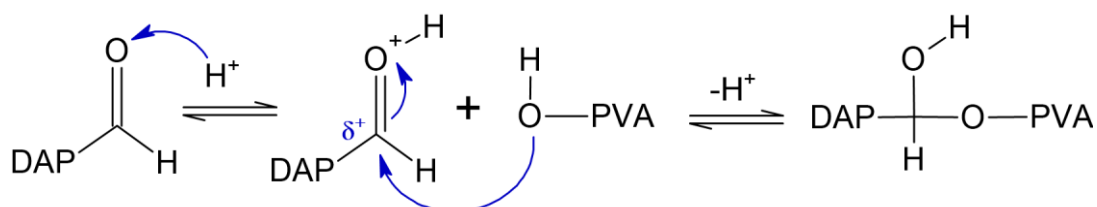

Figure 3 *The mechanism of hemiacetal bond formation between PVA and DAP*[31]

In general, a predetermined amount of PVA was dissolved in water and heated. Subsequently, the acidic catalyst (1.3 M HCl), and a given amount of crosslinker were added [31,66]. For the PVA/DAC hydrogels for transdermal drug delivery, 0.25% a 1% of the crosslinker were added. In the second study, 0.1% and 1% were used for DAC, DXI, and DXA, while 0.25 % and 2.5 % were for DAH, which has a lower density of -CHO groups. The resulting reaction mixtures were mixed thoroughly and poured onto Petri dishes (with a diameter of 140 mm) and dried at 30 °C until a constant weight was reached. The thin films obtained were washed with water to eliminate any non-crosslinked material, and circular samples were cut out.

6.3 DAPs and hydrogel characterization methods

FTIR, degree of oxidation (DO), Gel Permeation Chromatography (GPC), and dynamic light scattering (DLS) techniques were used to characterize specific crosslinkers, including DAC, DAH, DXI, and DXA. The cytotoxicity of crosslinkers was done in cooperation with Prof. Humpolíček at CPS. The characterization of DAPs are described in more detail, see [31]

Several techniques were used to investigate the characteristics of the prepared hydrogels, including network parameters, viscoelastic properties, BET, and SEM analysis, see references [31,66] for more details. In addition, drug release kinetics and transdermal absorption were measured for the PVA/DAC hydrogels for transdermal drug delivery (see section 7.1). For the role of DAP crosslinker structure in PVA hydrogels (section 7.2), the crosslinker structure, molecular weight, aldehyde group density, and size of the formed crosslinker nano-assemblies were studied. Cytotoxicity at CPS in collaboration with a group of Prof. Humpolíček at CPS was determined for all prepared hydrogels.

7. RESULTS AND DISCUSSION

A variety of combinations of hydrogels were successfully prepared and analyzed. The results, discussions, and conclusions will be analyzed separately for each type of study followed below.

7.1 PVA/DAC hydrogels for transdermal drug delivery

7.1.1 Preparation of the PVA/DAC hydrogels

Four different PVA/DAC hydrogels were prepared with varying concentrations of DAC and molecular weights of PVA, as shown in Table 1. Hydrogel samples are shown in Fig 4. Due to the poor physical properties of sample L-31, which were attributed to crosslinker concentrations and low PVA molecular weight, only network parameters were examined. The three other types of samples, L-130, H-130, and H-31, were, however, successfully characterized using the previously mentioned techniques (6.3).

Table 1 *Designation of PVA/DAC samples, M_w of PVA used and their composition[66].*

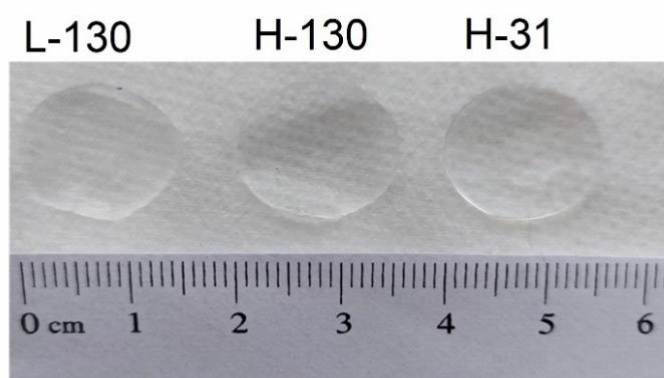| Sample	PVA M_w (kDa)	PVA (g)	DAC (wt.%)	DAC (g)
L-31	31	10	0,25	0,025
L-130	130	10	0,25	0,025
H-31	31	10	1	0,1
H-130	130	10	1	0,1

Figure 4 *Photograph of PVA/DAC samples[66]*

7.1.2 Characterization of the prepared hydrogels

Network parameters

The Flory-Rehner equilibrium swelling theory was used to estimate the network parameters of the hydrogels,[22] for details see relevant works[54,67].

The swelling and equilibrium water content (EWC) of PVA/DAC hydrogel samples (L-130, H-130, L-31, H-31) depend on the amount of crosslinker and the M_w of PVA (Table 2). Generally, a lower amount of crosslinker and a lower M_w of PVA lead to greater swelling and EWC. Thus, sample L-31 has the largest swelling, equal to almost 80-times of its dry mass. On the other side, sample H-130 swells only about 3.5-times. In contrast, the gel fraction grows when the concentration of DAC and M_w of PVA increase, therefore sample H-130 shows the largest gel fraction and sample L-31 the smallest. On the other hand, increasing the M_w of PVA decreases M_c (increases ρ_c) in the H-series (1% of DAC), but the opposite trend is observed in the L-series (0.25% of DAC). The difference is probably caused by differences in residual physical interactions, such as chain entanglements and hydrogen bridge networks between PVA macromolecules, as well as chemical crosslinks between PVA and DAC[54]. In particular, for the H-130 sample, where longer PVA chains offer significantly more crosslinking hotspots, it is probable that chemical crosslinking is more pronounced. Overall, the amount of crosslinker DAC plays a significant role in the network parameters of hydrogels, but the M_w of PVA further emphasizes this relationship.

Table 2 *Network parameters calculated for the PVA/DAC hydrogel samples[66]*

Sample	Swelling (%)	*EWC* (%)	Gel fraction (%)	M_c (g/mol)	ρ_c (µmol/cm^3)	ξ (Å)
L-31	7900 ± 800	99 ± 1	12 ± 1	12380 ± 20	103 ± 1	508 ± 17
H-31	707 ± 17	88 ± 1	48 ± 1	6410 ± 160	198 ± 5	169 ± 4
L-130	1150 ± 90	92 ± 1	59 ± 2	20700 ± 1900	62 ± 6	350 ± 30
H-130	351 ± 6	78 ± 1	89 ± 1	2890 ± 90	440 ± 14	93 ± 2

Viscoelastic properties

The dependence of storage modulus (G′) and loss modulus (G″) on angular frequency is given in Figure 5A and 5B. According to Figure 5A, the G′ values of the PVA/DAC hydrogel samples range from about 2100 Pa for sample H-130 to about 150 Pa for sample L-130. Corresponding G″ values range from about 190 Pa to 4.3 Pa. The crosslink density of PVA/DAC hydrogel samples clearly affects the G′ and G″ values, which are higher for denser mesh and lower for sparser mesh because the first type has a higher elasticity than the other one, which has more viscous behavior.[67] The L-130 sample with the lowest crosslink density displays the lowest G′ and G″ values, indicating more viscous-like behavior, while the most elastic is sample H-130. Viscoelastic properties of the hydrogels are similarly influenced by the M_w of PVA as lower M_w leads to lower G′ and G″ values, as can be seen from a comparison of H-31 and L-130 samples. The decreased M_w of PVA resulted in a nearly 70 % decrease in G′ values.

The complex dynamic modulus (G*) (Figure 5C) and damping factor (tan δ) (Figure 5D) show analogous correlations with the amount of crosslinker and M_w of PVA. Sample H-31, prepared with the same amount of crosslinker as H-130, has viscoelastic properties closer to L-130, highlighting the significant impact of the PVA matrix on hydrogel rheological properties.
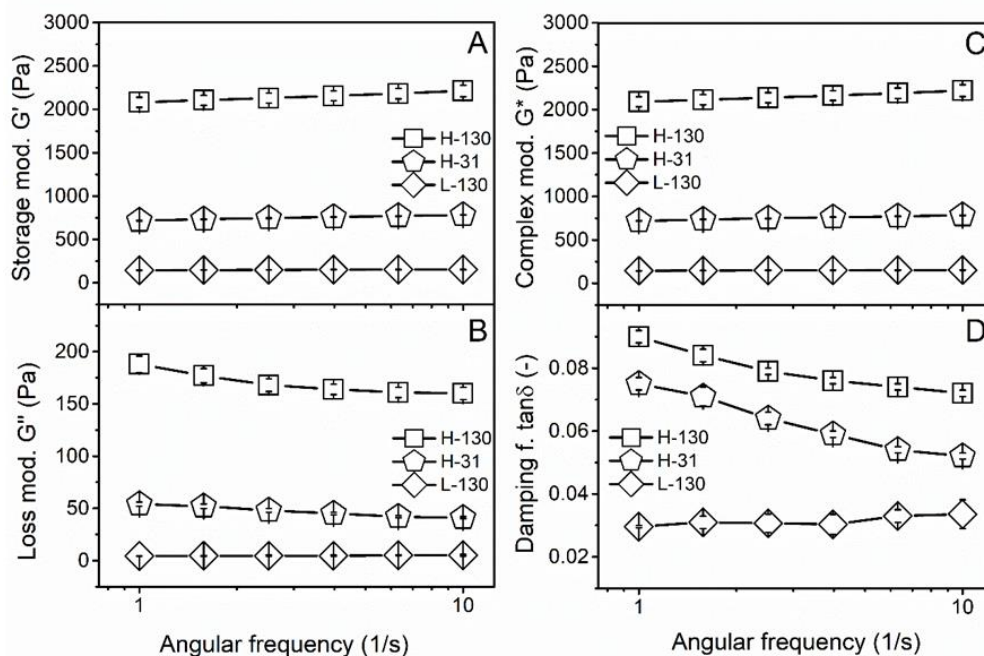

Figure 5 *Dependence of the G′ (part A) and the G″(part B) of PVA/DAC hydrogel samples on the angular frequency and dependence of the calculated complex modulus (G*, part C) and the damping factor (tanδ, part D) on the angular frequency*[66].

BET and SEM analysis

PVA/DAC hydrogels were lyophilized and their specific surface area (α_{BET}), total pore volume (V_p), mean pore diameter and adsorbed volume of nitrogen (V_a) was measured, see Fig. 6. In comparison to samples H-130 (2.0 ± 0.1 m²/g) and H-31 (2.2 ± 0.1 m²/g), sample L-130 has a α_{BET} value that is an order of magnitude higher (31.1 ± 0.9 m²/g) (Figure 6A). The results demonstrated that decreasing DAC concentrations significantly increased the hydrogels' specific surface area (BET), total pore volume (V_p), and V_a, with sample L-130 displaying the highest values (Figure 6). This can be explained by the extent of cavitation induced by the lyophilization process, which is indirectly connected to the hydrogel's capacity to absorb water. Interestingly, the mean pore diameter did not follow the same trend, with the H-series cryogels having fewer larger pores and L-130 containing a larger number of smaller pores. This is attributed to the molecular weight of the PVA used, which influences the mean pore size. SEM confirmed that the surface of the L-130 cryogel was highly porous in agreement with α_{BET} values, while the H-31 sample had slightly larger surface pores than the H-130 sample (Figure 6C).
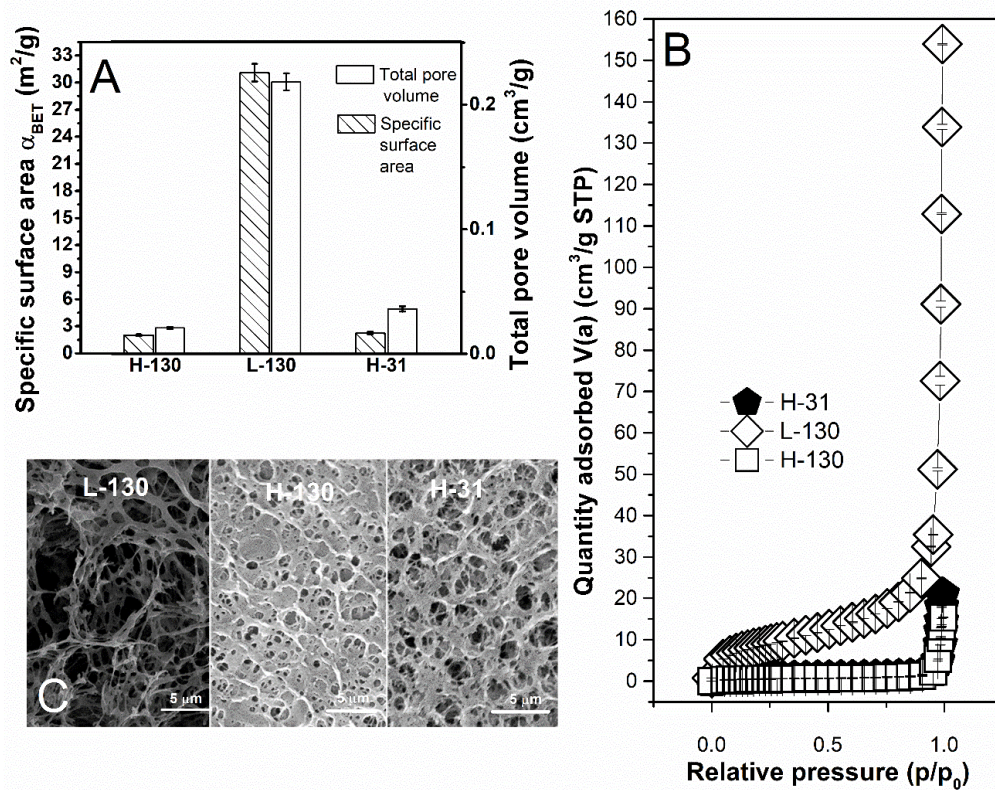

Figure 6 *The specific surface area α_{BET}, and total pore volume (V_p) of the prepared PVA/DAC cryogels (part A), the dependence of the amount of nitrogen adsorbed per mass of the cryogels on the relative pressure p/p_0 (part B), and SEM images of individual PVA/DAC samples taken at a magnification of 30.000 (part C)* [66].

Cytotoxicity

The biological evaluation was performed in collaboration with a group of Prof. Humpolíček at CPS. It consisted of two parts. Firstly, the cytotoxicity of hydrogel extracts in culture media was determined according to ISO 10993-12.[31,66] Secondly, the cell growth and morphology in the presence of hydrogels were observed, both in the media and directly on the gel surface.

The cytotoxicity of hydrogel extracts in culture media was determined and all materials were found to be non-toxic according to ISO 10933-5 (Figure 7).
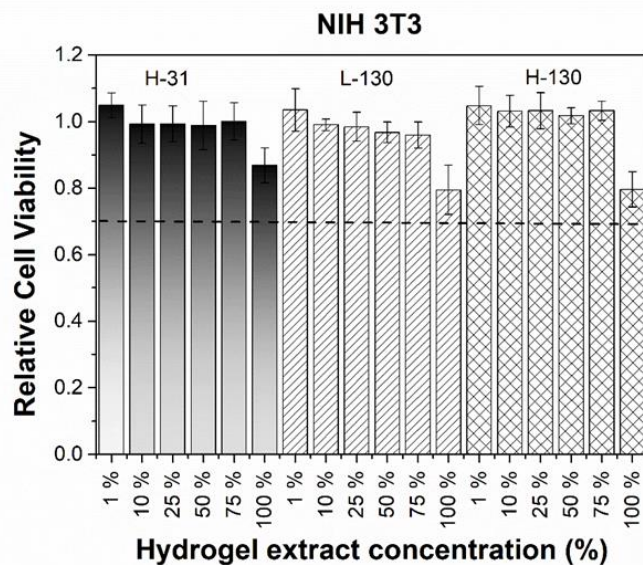

***Figure 7** Various amounts of PVA/DAC hydrogel extracts and their relative cell viability[66]*

The effect of hydrogel samples on cell growth and morphology was investigated by incubating samples with an NIH-3T3 mouse fibroblastic cell line for 96 hours. The MTT assay and microscopic observation were used to quantify cell viability and morphology. The results showed that the presence of hydrogel samples had no significant effect on cell growth or morphology. The cells reached confluence at the same time and their viability was the same as for cells not treated with hydrogels (Figure 8, top). Additionally, the fibroblasts retained their typical elongated shapes (micrographs in Figure 8, bottom), and no degradation of hydrogels was observed during the tests or after one week of in vitro conditions. To assess the cells' growth and morphology in direct contact with the hydrogel, however, was impossible since they did not adhere to the hydrogel surface. Although the results suggest that hydrogel films are suitable for topical applications, additional tests are necessary to claim biosafety *in vivo*.
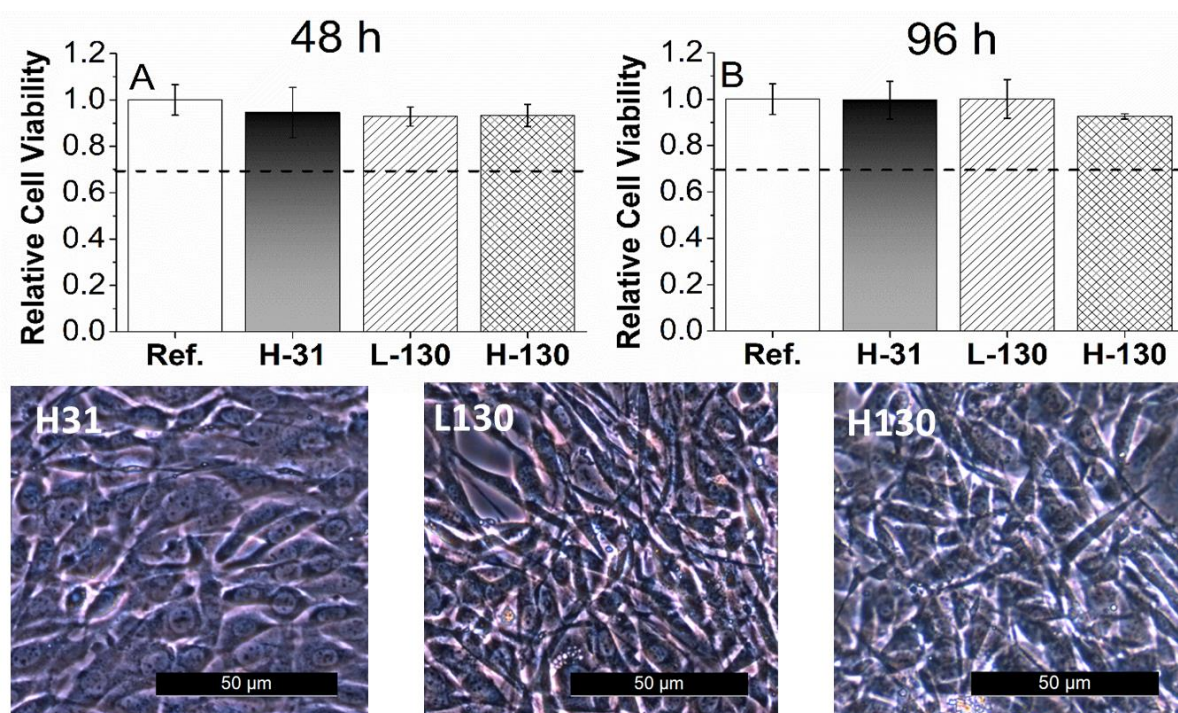
Figure 8 *Relative cell viability of cells incubated in the presence of PVA/DAC for 48 and 96h and micrographs of cells after 96 h[66]*

Drug release and transdermal absorption of prepared PVA/DAC hydrogels

The kinetics of release and transdermal absorption of two model drugs, caffeine and rutin, were investigated using a UV-VIS spectrometer at 353 nm (rutin) and 273 nm (caffeine)[31,66].

The release rates of caffeine, which is a relatively small molecule, were identical for all three hydrogel materials tested (Figure 9B). For larger rutin molecules, there were minor differences in the release kinetics among the samples, with the fastest release observed in the H-31 sample (Figure 9A). These differences may be related to the lower molecular weight of PVA and its influence on pore size, but further tests would be needed to confirm this observation. The relatively low thickness of the hydrogel films may have minimized the impact of the hydrogel network on drug release rates. This could be improved by employing thicker films or changing the drug loading process. However, the observed release kinetics, which includes fast initial release rates (up to 80–90% of compounds released in 8 h), seem to be well suited for topical drug delivery applications, where the expected time of application is in the order of hours. An analysis of these data was also conducted using the mathematical Korsmeyer-Peppas model (see section 2.2). The values of the exponent n are presented in Table 3. The results suggest that the release mechanism occurs based on Fickian diffusion.
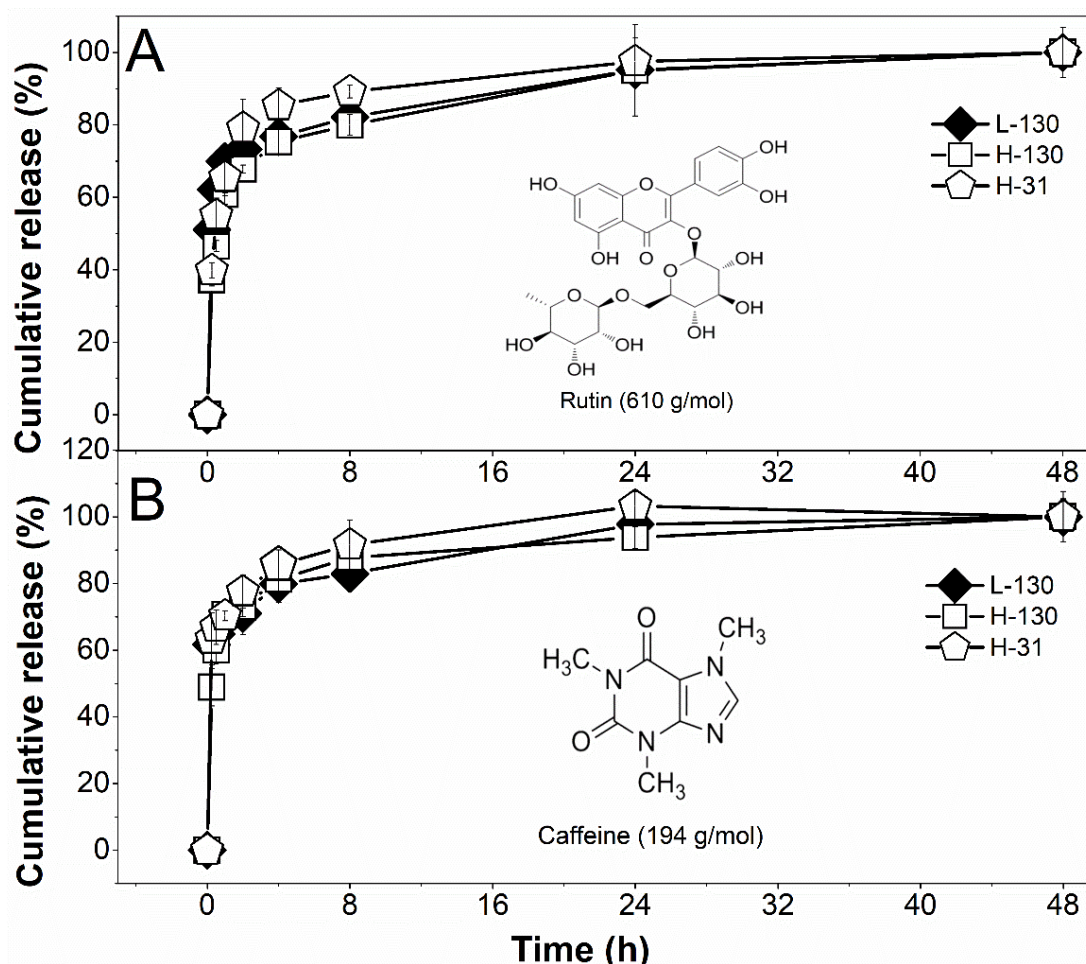
Figure 9 *Cumulative release of rutin (part A) and caffeine (part B) from PVA/DAC hydrogels*[66]

Table 3 *Results of the release exponent n according to the Korsmeyer-Peppas model*

	RUTIN	**CAFFEINE**
SAMPLE	Exponent n	Exponent n
L-130	0.12 ± 0.03	0.14 ± 0.02
H-130	0.17 ± 0.03	0.163 ± 0.009
H-31	0.2 ± 0.1	$0,1020 \pm 0.0006$

Transdermal absorption

The skin absorption tests for caffeine were conducted following the OECD Test Guideline. The measurement was tested using an automated diffusion cell system, with a continuous flow of receptor liquid. The amount of caffeine absorbed through the skin was analyzed by liquid chromatography using an HPLC chromatograph equipped with a UV-VIS detector using a wavelength of 272 nm [31,66].

Although all samples were loaded using the same technique, the total caffeine dose differs between samples due to their different EWC, gel fractions, and equilibrium swelling. Sample L-130 had the highest caffeine load (around 900 µg), whereas sample H-130 was able to absorb a small amount (about 500 µg), (Table 4). Aqueous caffeine solution containing 250 µg of caffeine was used as a reference.[69].

Table 4 *Caffeine amount present in the samples (µg) and the dose of caffeine per cm^2 of skin[66].*

Sample	Total dose of caffeine (µg)	Dose per cm^2 (µg/cm^2)
L-130	896 ± 8	1134 ± 10
H-31	660 ± 6	832 ± 7
H-130	495 ± 1	625 ± 1
Reference	250	320

Results showed that penetration of caffeine through the skin was slow, with only between 0.07% and 0.2% of the total dose crossing the skin barrier within 24 hours (Figure 10 C, D). According to Trauer et al.[69], this is due to an absence of blood supply to the skin during the *in vitro* study. Caffeine absorption through the skin of a living organism would be much faster. Moreover, the hydrophilic nature of caffeine presents a significant challenge to its penetration through the stratum corneum. This is consistent with the results of several other studies, including those by Bonina et al.[70], Santander-Ortega et al.[71], and Pilloni et al.[72], where it was also discovered that caffeine transdermal absorption was relatively low, typically in the range of tenths of a percent of the applied dose, despite of the various carriers used. Despite this low amount, the L-130 sample, which had the lowest elasticity and best adhered to the skin, had the highest overall amount of caffeine absorbed (1400 ng/0.15%), whereas only 350–450 ng (0.06-0.07%) of caffeine was absorbed from H-series samples over 24 hours. The amount of caffeine permeated from the L-130 sample is approximately twice larger than from H-series samples, Fig. 10 C, D.

The hydrogel L-130 was identified as the most promising candidate for transdermal delivery of biologically active substances without the need for skin-penetration enhancers. Its physical properties allow easy handling and adherence to the skin, which enhances its transdermal drug delivery properties. Next, the role of crosslinker structure and properties was examined.
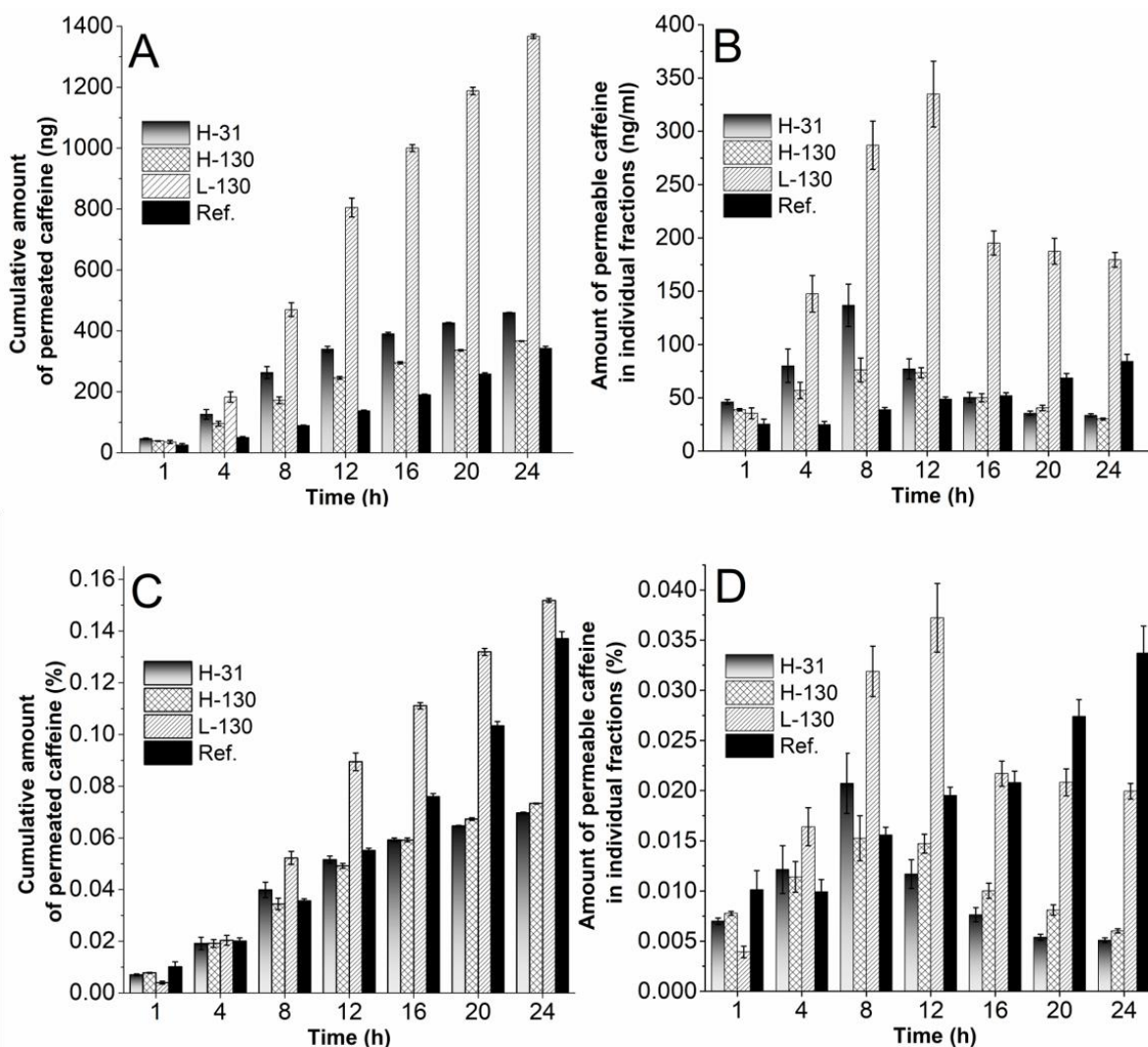
Figure 10 *The cumulative amount of penetrated caffeine [ng] (part A), the time-dependent quantity of permeated caffeine [ng/mL] (part B), the total amount of transdermally absorbed caffeine relative to applied dose [%] (part C), and the time profile of caffeine absorption relative to applied dose [%] (part D)* [66].

7.2 The role of DAP crosslinker structure in PVA hydrogels

7.2.1 Preparations of PVA/DAPs hydrogels

The hybrid hydrogel samples prepared in this study are designated as PVA/DAP and are categorized and named DAC, DXI, DXA, or DAH based on the type and concentration of the crosslinker used, with -L and -H indicating lower (0.1/0.25 wt%) or higher (1/2.5 wt%) concentrations, respectively. Some of the swelled PVA/DAP hydrogel samples (H series) were also subjected to a 3-hour treatment in closed reaction flasks with demineralized water heated to 70 °C (labeled as DAP-HT), to enhance the role of chemical crosslinks by disrupting hydrogen bonding in residual crystallites formed between PVA chains during drying. Individual PVA/DAPs hydrogels are shown in Figure 11.

Figure 11 *Photographs of PVA/DAPs hydrogels samples*[31]

7.2.1 Characterization of DAP crosslinkers

DAPs were prepared as described in (6.2). Conditions of periodate oxidation were set to obtain fully oxidized materials[34,68]. Regarding the differences between DAPs, the dialdehydes of cellulose, dextran, and dextrin are composed of similar building blocks (i.e. oxidized glucopyranose units) and thus share very similar structural patterns. However, the four DAPs retain unique back bone and side group structural features of their source compounds and the properties of DAPs are to a large extent given by the architecture and characteristics of source polysaccharides, they differ significantly. Therefore, the molecular weight, DO, FT-IR, size of nano-assemblies formed by DAPs in the solution and their cytotoxicity were analyzed before the preparation of hydrogels.

The gel permeation chromatography analysis (GPC)

To determine the molecular weight of the prepared dialdehydes, they were converted to corresponding doubly-oxidized dicarboxylated derivatives (DCP) namely DCDXA - dicarboxy dextran, DCH - dicarboxy hyaluronate, DCDXI - dicarboxy dextrin, and DCC - dicarboxy cellulose. This conversion was necessary, as DCPs are more stable and have a better-defined composition

compared to DAPs, which tend to form hemiacetals and self-crosslinks. This method has also been used previously with good results[68]. To analyze the molecular weight of the samples, a Waters HPLC Breeze chromatographic system with a refractive index detector was used. The highest M_n is found in the DXA at 30 kDa, followed by the DAH at 21 kDa, while the M_n in the DXI and DAC is nearly identical at 12 kDa, see Table 5 for more details.

Table 5 *Number average molecular weight (M_n), weight average molecular weight (M_w), polydispersity index (PDI), degrees of polymerization (DP) of dicarboxy and dialdehyde polysaccharides, their DO, and molar amount of –CHO groups per unit of crosslinker mass (n_{-CHO})* [31]

DCP	M_w (kDa)	M_n (kDa)	PDI	DP	DAP	M_w (kDa)	M_n (kDa)	DO (%)	n_{-CHO} (mmol/g)
DCDXA	84.8	44.1	1.92	420	DXA	58.0	30.2	85±4	12.3±0.4
DCH	47.8	24.8	1.92	103	DAH	41.2	21.4	99±6	5.0±0.3
DCDXI	36.9	16.9	2.17	157	DXI	25.2	11.5	98±1	12.5±0.2
DCC	31.2	16.9	1.84	132	DAC	21.2	11.5	95±2	12.4±0.3

The degree of oxidation

The DO (degree of oxidation) of each DAP, which is defined as a percentage of the total amount of basic structural units that were oxidized to dialdehydes, was determined using oxime reaction[73]. DAC, DAH, and DXI were nearly fully oxidized with a DO greater than 95%, while the maximum DO of DXA was limited to around 85% due to the presence of 15% of oxidation-resistant branched units. This corresponds to: 12.5 mmol/g of -CHO groups in DAC and DXI, while DXA oxidized to 85% contains 12.3 mmol/g of -CHO groups (Table 5). The presence of oxidation-resistant N-acetyl-D glucosamine units in DAH reduces the maximum -CHO content to 5.0 mmol/g, which is 2.5 times lower than that of the tested homoglycans. Therefore, the amount of DAH crosslinker used in hydrogel preparation was increased by 2.5 times to better assess the impact of molecular weight, structure, and -CHO group density of individual DAPs.

Dynamic light scattering (DLS)

The hydrodynamic radii (d_h) and zeta potentials (ζ) of DAP nano-assemblies formed in their solutions were investigated using DLS (Table 6). The linear DAP molecules (DAC, DAH) formed larger nano-assemblies compared to the branched crosslinkers, despite these having the same (DXI) or even higher (DXA) M_n than their linear counterparts. DAH created the largest nano-assemblies, whereas DAC, despite having an approximately 3x lower molecular weight (M_n), produced outcomes comparable to those of DXA. Interestingly, the size of DXI nano-assemblies was almost 1.5 times smaller than that of DAC with the same M_n. With

a polydispersity between 0.35 and 0.4, the size distribution of the DAC, DXI, and DAH nano-assemblies was relatively uniform. The size distribution of DXA assemblies, however, was distinctly bimodal, with the majority (approximately 80%) of the assemblies being larger (d_h 270 nm) and the minority (about 20%) being smaller (20 nm).

Table 6 *The hydrodynamic radii (d_h) and zeta potentials (ζ) of DAPs*[31]

sample	d_h (nm)	ζ (mV)
DXA	267 ± 19 (20 ± 3) *	-14.6 ± 1.1
DAH	308 ± 1	-31.0 ± 1.9
DXI	170 ± 11	-23.6 ± 1.5
DAC	250 ± 30	-23.6 ± 1.1

*DXA sample has a bimodal size distribution

Regarding the stability of colloids, their ζ-potential values ranged from -15 mV for DXA to -31 mV for DAH. This is expected because DXA is partly composed of less polar, non-oxidized anhydroglucose units, whereas DAH has one carboxylic group per each fundamental structural unit increasing its negative charge. The stability of the colloids was confirmed by repeating the DLS and ζ-potential measurements one week after their preparation, which gave essentially the same results.
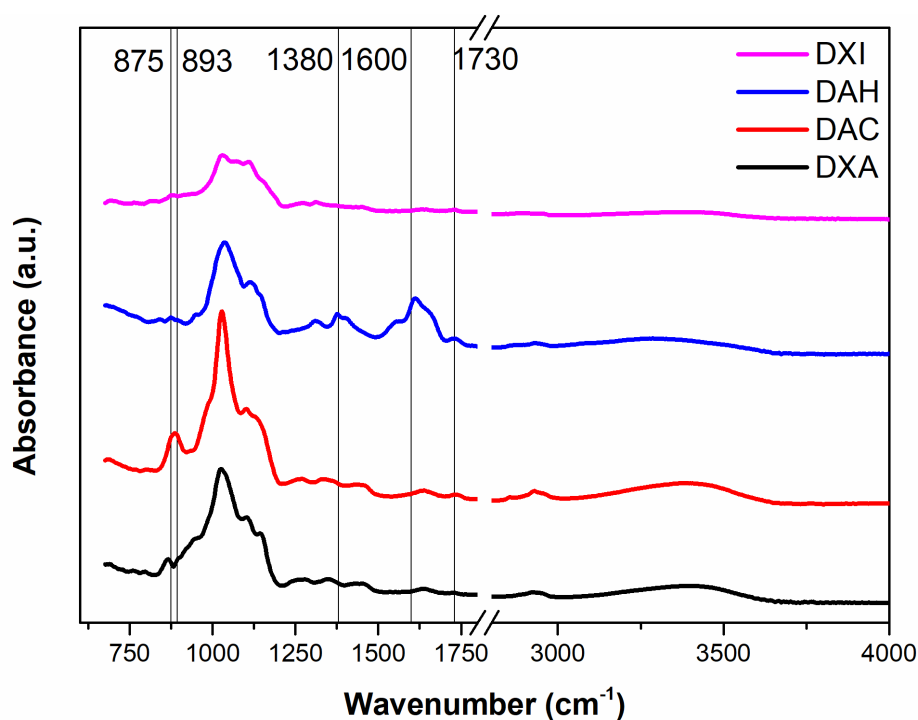
Figure 12 *FT-IR spectra of DAPs*[31]

FTIR analysis

The IR spectra of all DAPs show distinctive absorption bands around 1730 cm^{-1} (C=O vibration from -CHO) and 875 cm^{-1} (C-O-C vibration), indicating the presence of both free aldehyde groups and newly formed hemiacetal groups as you can see in Figure 12. The spectrum patterns of DAC, DXI and DXA crosslinkers are similar because they are all formed from oxidized glucopyranose units. On the other hand, DAH shows distinctive absorption bands that are connected to the existence of -COOH groups in the glucuronic unit, such as an asymmetric valence -COO vibration at around 1600 cm^{-1} and a deformation vibration -OH from COOH at around 1380 cm^{-1}. The absence of the glucuronic acid fingerprint vibrational band at 893 cm^{-1} in the DAH spectra suggests that the C2-C3 bond has been broken as a result of quantitative oxidation.

Cytotoxicity

In collaboration with a group of Prof. Humolíček at CPS, all DAPs were found to be non-cytotoxic up to 0.1 mg/mL, and some even supported cell growth at lower concentrations (Figure 13). DAH, DXA, and DAC were the least cytotoxic, while DXI was the most cytotoxic. The number of reactive -CHO groups did not correlate with the cytotoxicity of the cross-linking agents, however, which may be due to the size of their nano-assemblies and related differences in transport through the cell wall. Overall cytotoxicity of crosslinkers is relatively low compared to other crosslinking agents. To put these results into a proper perspective, a comparison to glutaraldehyde (GA) was performed. GA was found to be highly toxic even at the lowest concentration used (0.05 mg/mL). Speer et al. even reported 99% inhibition of 3T3 fibroblast growth at a GA concentration of 0.003 mg/mL[6]. DAPs are thus several orders of magnitude less toxic.
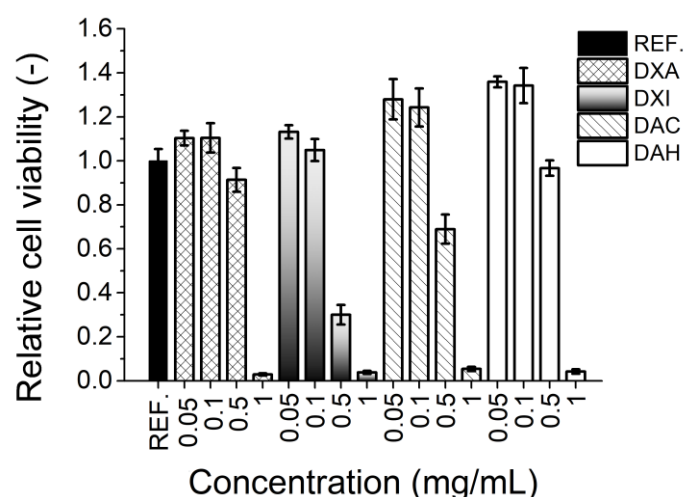

Figure 13 *Relative cell viability containing 0–1mg/mL of DAP for 24 h[31]*

Crosslinkers were subsequently used to prepare hydrogels, whose properties are discussed in the following section.

7.2.2 Characterization of prepared PVA/DAP hydrogels

Network parameters

Network parameters of all types of PVA/DAP hydrogel samples were calculated according to Flory and Rehner[22]. The DAH-H sample showed the largest swelling among the H-series samples (approximately 225%), followed by the DXI-H and DAC-H samples, which both swelled by about 200%, and the DXA-H sample, which swelled by 170% (Figure 14). Similar trends are observed for average molecular weight between crosslinks M_c and the mesh size ξ, whereas the crosslink density (ρ_c) increases in the opposite order (DXA-H has the highest crosslink density).
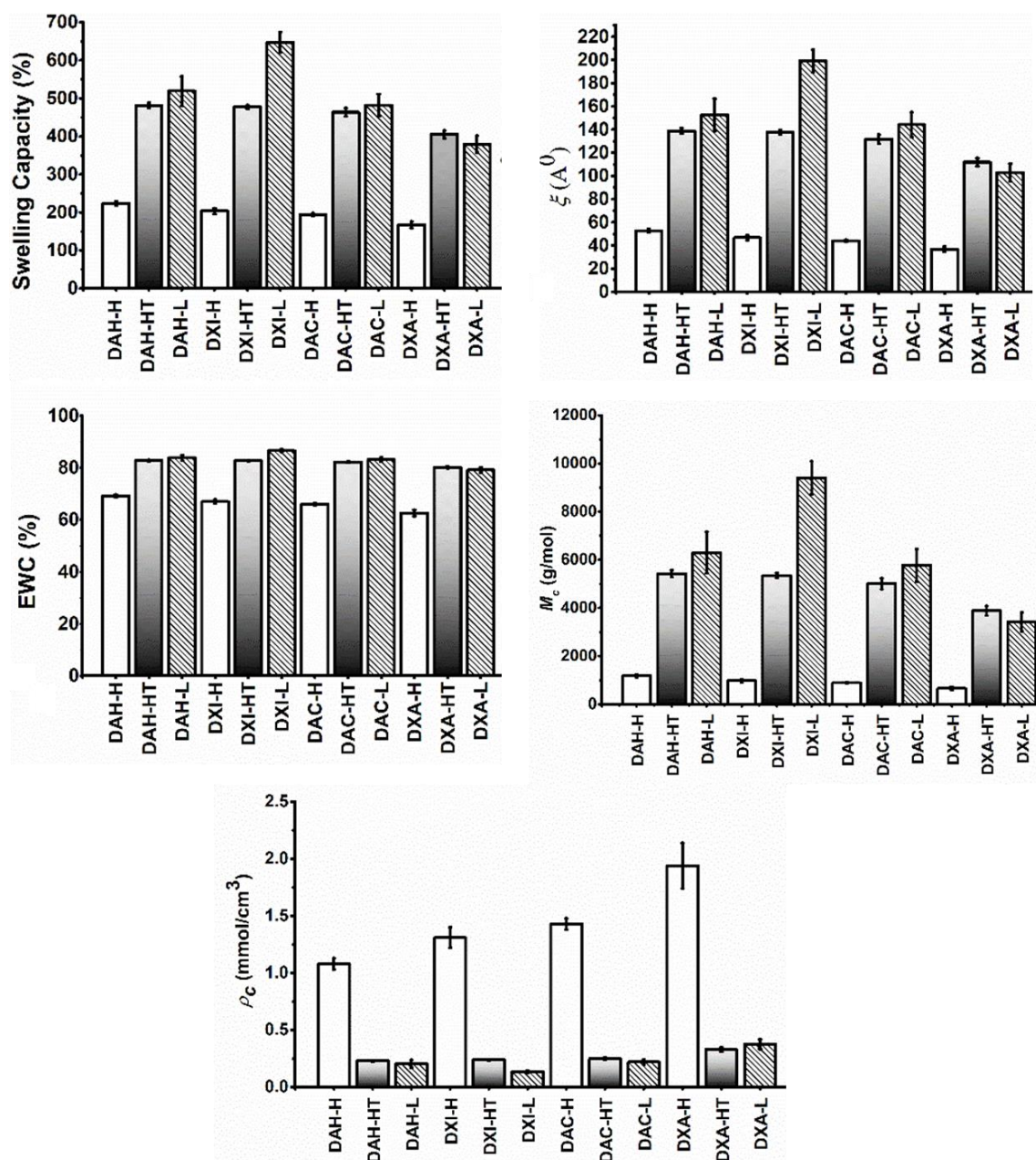
***Figure 14** Network parameters calculated for PVA/DAP hydrogels[31]*

Heat treatment of the samples leads to a significant increase in hydrogel swelling, up to 480% for DAH-HT. DXA-HT sample had the lowest swelling of 400%. The H-series hydrogels followed the same trend. As a result of heating, other network characteristics also displayed a significant decrease in crosslink density, which is probably due to the disruption of PVA's physical crosslinks, which are created during the preparation of hydrogel films. In the L-series, the highest swelling was observed for DXI (620%), followed by DAH (500%) and DAC (480%), while DXA had the lowest swelling (420%).

Viscoelastic properties

Graphs in Figure 24 show the storage (G') and loss (G'') modules of various PVA/DAPs hydrogel samples as a function of different angular frequencies. The higher G' values than G'' values in all samples demonstrated a higher degree of elasticity than viscosity, which corresponds to hydrogel formation. The G' values for the H-series samples range from 3500 Pa for the DXA-H sample to 6500 Pa for the DXI-H sample (Figure 15). Note, that the DXA-H sample had the highest crosslink density but the lowest G' value. This issue is likely caused by the bimodal size distribution of DXA nano-assemblies, see below. G'' values followed the same trend as G', with DXI having the highest and DXA having the lowest values. The same trend was reflected in the damping factors, with DXI and DAC being the most elastic, and DAH and DXA more viscous-like (Fig 16).
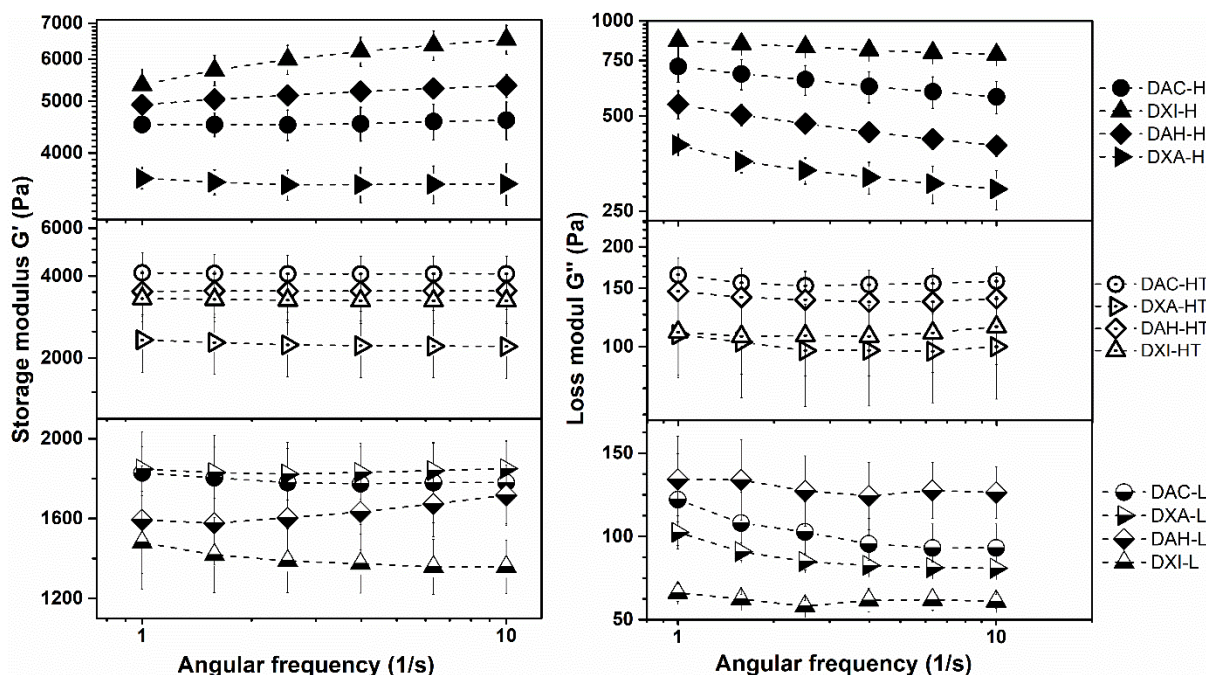

Figure 15 *Dependence of storage modulus and loss modulus of PVA/DAPs on angular frequency*[31]

Due to the loss of crosslinking caused by heating, all samples in the HT series showed a decrease in G', G'', and tan δ, with DAC-HT having the smallest decrease and DXI-HT getting the greatest decrease.

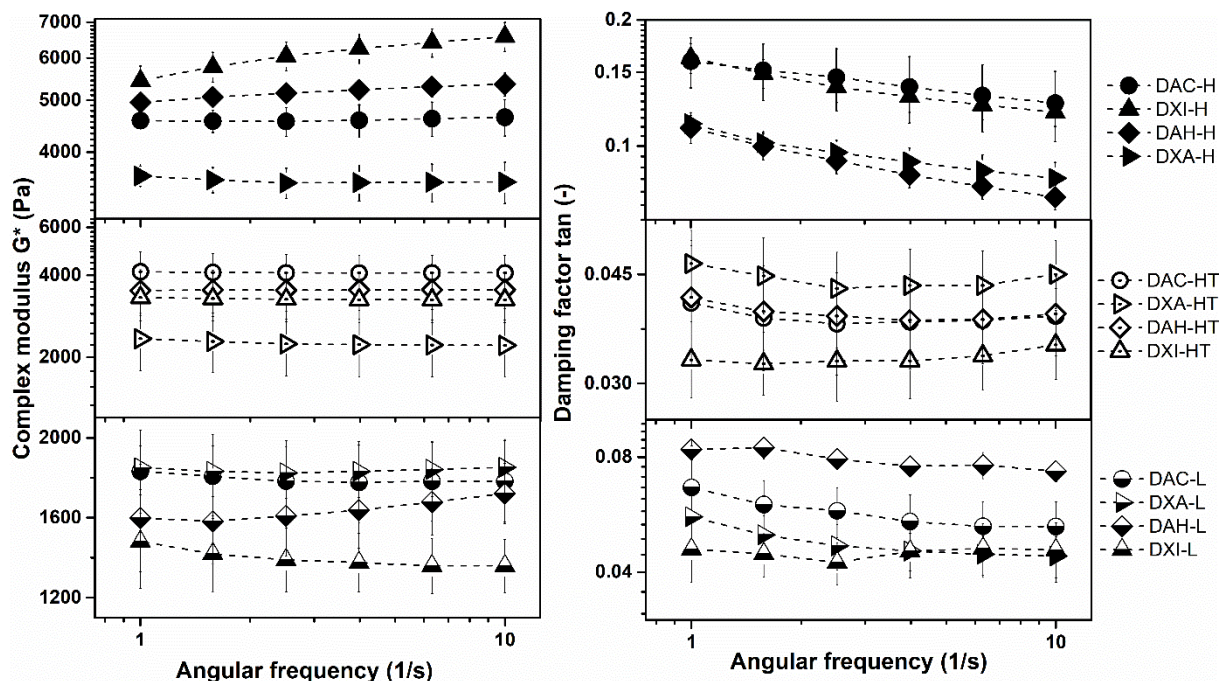**Figure 16** *Complex modulus G* and damping factor tan of PVA/DAPs depend on the angular frequency[31].*

The G′, G″, and tan δ, of the L-series samples were similarly decreased, with DXI-L showing the largest decrease and DXA-L showing the smallest decrease in storage modulus compared to the H-series. The DAH-L showed the lowest decrease in G″ (and thus the highest overall tan δ) among the L-series samples. The values for the other L-series samples were mostly comparable within experimental error.

BET and SEM analysis

The porosity of PVA/DAPs was analyzed using BET and SEM techniques, and the results are shown in Figure 17 for BET and Figure 18 for SEM. The L-series samples were found to be more porous than the H-series samples. Among the H-series samples, DAH-H showed the highest specific surface area (α_{BET}) (3.9 m^2/g) and total pore volume (V_p) values (0.038 cm^3/g), whereas DAC-H had the lowest. The mean pore diameter (d_m) was also found to be highest in DAH-H (~35 nm), and lowest in DAC-H (~27 nm). In all cases, heating the samples increased the α_{BET} and V_p values, with DAH-HT remaining the most porous material. The DXI-L sample was found to be the most porous sample overall, with DXA-L being the least porous of the L-series samples. The decrease in crosslinker amount led to a significant increase in porosity. SEM images of fracture surfaces of lyophilised hydrogels in Figure 18 also support these findings.
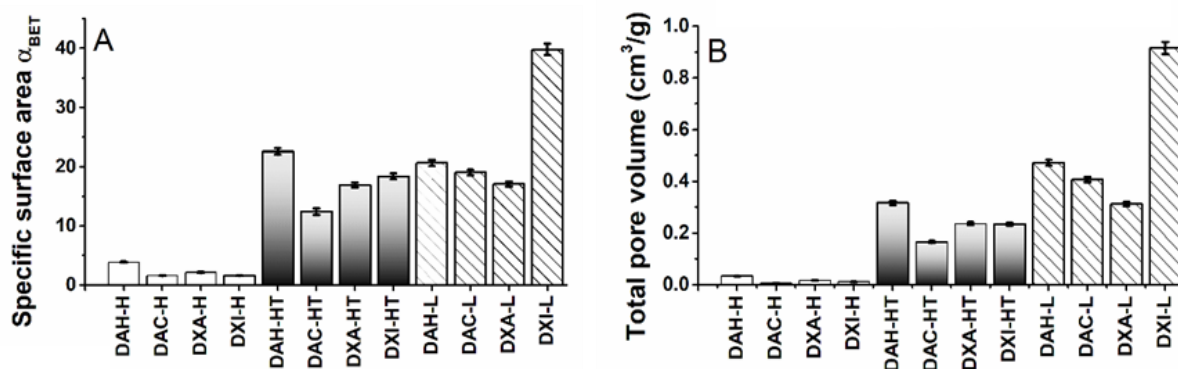
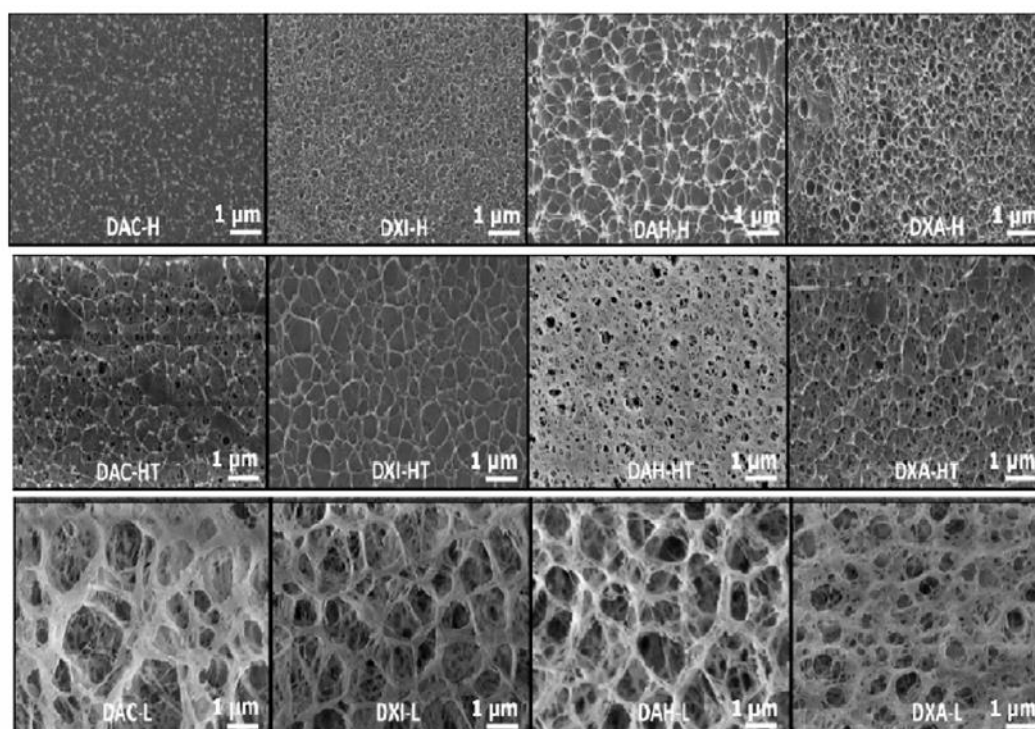*Figure 17* *Specific surface area (part A), total pore volume (part B) of PVA/DAPs hydrogels[31]*

Figure 18 *SEM analysis of lyophilised PVA/DAPs hydrogels[31]*

Cytotoxicity

In collaboration with a group of Prof. Humpolíček at CPS, cytotoxicity was determined according to ISO 10 993-5, Figure 20 displays the results for 100% extracts from hydrogels. Hydrogel extracts are considered non-toxic if the relative cell viability is above 0.7, as indicated by the dashed line in Figure 20. It was discovered that the cytotoxicity of hydrogel extracts is influenced by both the amount of the crosslinker and the heating of the gel matrix. DAH and DXA-based hydrogels were found to be the least cytotoxic, while DAC and DXI-based hydrogels were found to be mildly cytotoxic in both L- and H-series. However, heat treatment of hydrogels significantly reduced the cytotoxicity of hydrogel extracts, especially for DXI.
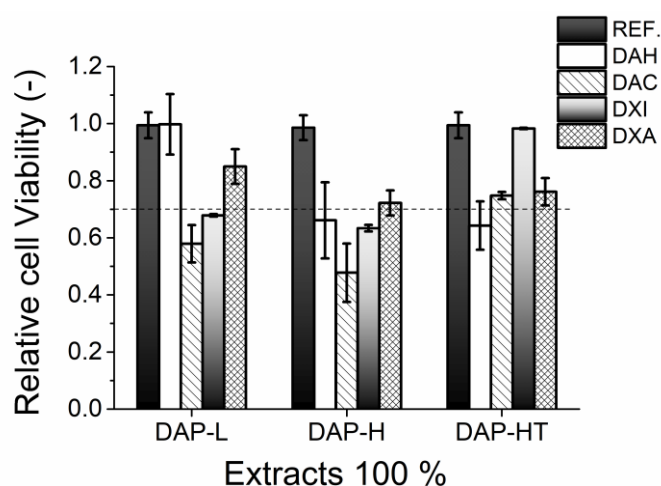
Figure 19 *Cytotoxicity of the PVA/DAPs extracts[31]*

7.2.3 Unraveling of DAP crosslinkers' effects in PVA matrix

Based on the obtained data, the following conclusions were reached.

DAC - DAC-based hydrogels have properties that indicate effective chemical crosslinking, such as high storage modulus and damping factors, as well as good retention of rheological properties even after heating and at low crosslinker concentrations, and the porosity of DAC xerogels is among the lowest across all series. The high –CHO group density and large DAC nanodomains, comparable to those of almost three times heavier DXA, contribute to the efficient crosslinking of distant PVA chains as schematically demonstrated in Figure 21. The presence of β-glycosidic bonds in DAC also enhances its crosslinking effectiveness by allowing efficient crosslinking of different PVA chains even by relatively close DAC units. The mild cytotoxicity of PVA/DAC hydrogel extracts is a disadvantage, but it can be improved by heating. In summary, DAC is an effective crosslinker for hydrogels but of limited biological application.

DXI - Although M_n, n_{-CHO}, and the chemical composition of DXI-based hydrogels are essentially comparable to those of DAC, their structural differences (branching) lead to significantly different characteristics. The properties of DXI-based hydrogels degrade rapidly after heating and at low crosslinker concentrations. The observed differences between DXI and DAC are most likely caused by the smaller size of DXI domains rather than molecular weight or -CHO group density. As a result, smaller regions of very high crosslink density are embedded in physically crosslinked PVA network hydrogels (Figure 21). DXI-based hydrogels are the least suitable for biomedical applications since they demonstrate one of the highest observed cytotoxicity of all tested species (but still mild). In conclusion, compared to other tested species, DXI-based hydrogels demonstrate characteristics that make them the least suited for crosslinking.

DAH - Because linear DAH macromolecules are based on heteroglycan, they can only be oxidized by periodate at glucuronic acid units. DAH thus contains fewer crosslinking hotspots per macromolecule compared to AGU derivatives. As a

34

result, the DAH forms a more loosely bound network than DAC, leading to high swelling, lower network density, high porosity, and moderate storage modulus in DAH-H hydrogels. However, DAH-based hydrogels maintain their properties better than DXI-based hydrogels. These do not degrade as quickly as those of DXI-based samples, and even perform similarly to DAC-based hydrogels at low crosslinker concentrations. This is likely due to the larger size of DAH nano-assemblies and possibly higher M_n of DAH macromolecules, which allows them to crosslink more distant PVA chains (Figure 21). DAH-based hydrogels showed the lowest cytotoxicity compared to other samples. In summary, DAH-based hydrogels have a more viscous character, lower cytotoxicity, and higher porosity than other hydrogels, indicatiing them for scaffolds in tissue engineering.

DXA - Due to their densest mesh, the DXA-based hydrogels should have the highest storage modulus and damping factors because they have the lowest swelling and highest crosslink density. However, this trend is only observed in the DXA-L sample, while the G′ values of DXA-H and DXA-HT are the lowest within their respective series. This unexpected behavior is attributed to the bimodal size distribution of DXA nano-assemblies, with the small domains (d_h ~20 nm) acting as a "secondary" crosslinker network, binding nearby PVA chains. The DXA hydrogels have lower cytotoxicity and better mechanical properties than DAH-based hydrogels, especially at low concentrations.
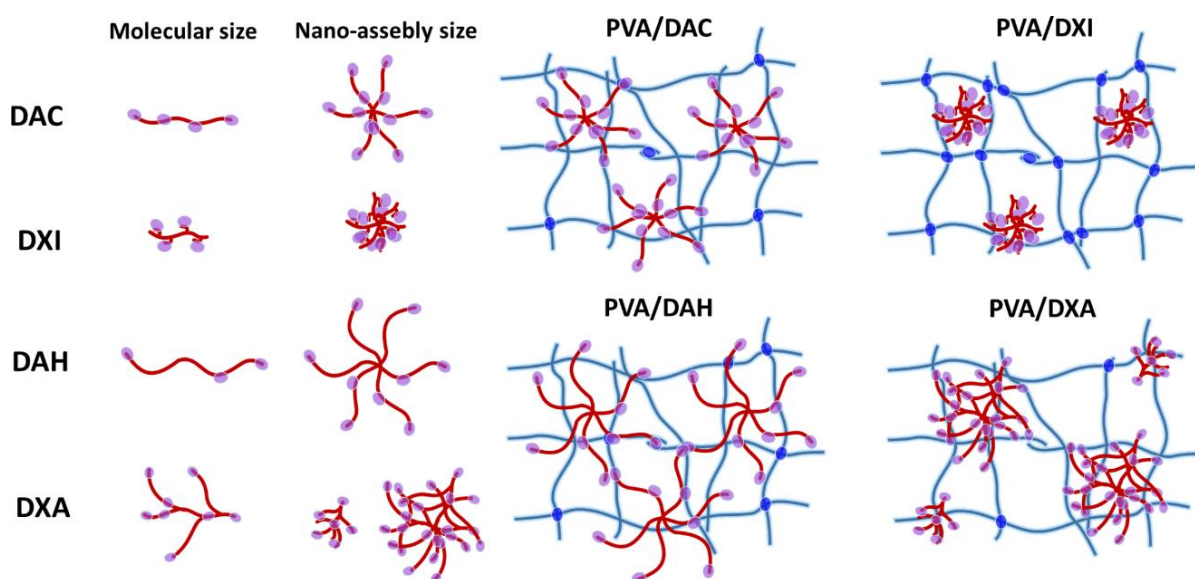

Figure 20 *The size of the crosslinker molecules, n_{-CHO}, hydrodynamic radii, and the predicted crosslinking mode of the PVA network are shown schematically. Crosslinking hotspots are shown in purple, and the PVA matrix's residual physical crosslinks are shown in blue. The number of crosslinking hotspots shown corresponds to the ratio of -CHO groups between crosslinker molecules, while the sizes of individual macromolecules and nano-assemblies reflect the observed M_n and d_h, respectively. For better clarity, the PVA matrix was represented uniformly, showing the same PVA concentration during the crosslinking[31]*

8. CONCLUSIONS AND CONTRIBUTION TO SCIENCE AND PRAXIS

The main outputs of my research include i) the preparation of PVA/DAC hydrogels and the study of the effect of the PVA matrix on their properties, and ii) the preparation of PVA/DAPs hydrogels and the study of the structure-function relationship of DAP crosslinkers. These results were published in Materials Science and Engineering: C and Carbohydrate Polymers [31,66].

The first contribution showed that the increased M_w of PVA affects the crosslink density and mesh size and improved hydrogel stability. These molecular-level changes have the greatest impact on equilibrium swelling capacity and viscoelasticity. On the other hand, DAC crosslinker concentration controls the specific surface area and total pore volume, while the PVA type affects the mean pore size. The amount of DAC crosslinker and M_w of PVA do not have a significant effect on the drug release rate, most likely because the investigated pharmaceuticals (rutin and caffeine) are small molecules and, therefore, sensitive to the nearest molecular environment, whereas the long-distance structural parameters do not influence their diffusion. In other words, the size of the molecules was very low in comparison with the hydrogel mesh. Through analytical data exploration, it has been verified that the kinetics of caffeine and rutin release can be described utilizing the Kosmeyer-Peppas mathematical model. It has been determined that the release mechanism of these substances is governed by the Fickian diffusion mechanism. All prepared hydrogel films were also non-toxic and therefore suitable candidates for transdermal drug delivery patches and wound dressings. As a result of high porosity, high water content, and excellent skin adhesion that improved the drug absorption, the hydrogel sample L-130 (L-low concentration of cross-linker, 130-highest M_w PVA) is the best for dermal patches and transdermal delivery of biologically active compounds.

The second contribution showed that the structural variances of the prepared DAPs have a significant effect on the properties of the prepared PVA/DAPs hydrogels. A lower density of -CHO groups leads to higher hydrogel swelling and porosity, but lower elasticity. Different macromolecular chain architectures can have a significant impact on hydrogel properties, as demonstrated by DXI and DAC having the same M_n. Hydrogels based on linear polysaccharides (DAC, DAH) are generally less affected by the decreased concentration of crosslinker or heat treatment while branching can have either positive (DXA) or negative (DXI) effects at lower concentrations depending on the size of the crosslinking nanodomains. Regarding the comparison of individual crosslinkers, DXA is the most effective crosslinker at low concentrations, resulting in hydrogels with low swelling and low cytotoxicity,

making it a promising alternative to DAH-based hydrogels for the preparation of biomaterials that require better physical properties.

This research underlines the importance of understanding the molecular structural factors that influence the final properties of the hydrogels, contributing to advances in biomedical material base solutions. The insights gained here encourage a balanced approach to hydrogel research, considering both chemical composition and physical properties, and stress out the practical implications of specific hydrogel formulations. These contributions can potentially guide the development of future medical products and lead to further improvements in the field of hydrogel healthcare materials. Continuing such research could help in optimising healthcare resources, enhancing patient recovery processes, and improving overall health care outcomes.

REFERENCES

(1) *Handbook of Biopolymer-Based Materials: From Blends and Composites to Gels and Complex Networks*; Thomas, S., Durand, D., Chassenieux, C., Jyotishkumar, P., Eds.; Wiley-VCH Verlag GmbH & Co. KGaA: Weinheim, Germany, 2013.

(2) *Biopolymers and Nanocomposites for Biomedical and Pharmaceutical Applications*; Sharmin, E., Zafar, F., Eds.; Polymer science and technology; Nova Biomedical: Hauppauge, New York, 2017.

(3) Chen, R.; Hunt, J. A. Biomimetic Materials Processing for Tissue-Engineering Processes. *J. Mater. Chem.* **2007**, *17* (38), 3974. https://doi.org/10.1039/b706765h.

(4) Ma, P. X. Biomimetic Materials for Tissue Engineering. *Advanced Drug Delivery Reviews* **2008**, *60* (2), 184–198. https://doi.org/10.1016/j.addr.2007.08.041.

(5) Tibbitt, M. W.; Anseth, K. S. Hydrogels as Extracellular Matrix Mimics for 3D Cell Culture. *Biotechnol. Bioeng.* **2009**, *103* (4), 655–663. https://doi.org/10.1002/bit.22361.

(6) Speer, D. P.; Chvapil, M.; Eskelson, C. D.; Ulreich, J. Biological Effects of Residual Glutaraldehyde in Glutaraldehyde-Tanned Collagen Biomaterials. *J. Biomed. Mater. Res.* **1980**, *14* (6), 753–764. https://doi.org/10.1002/jbm.820140607.

(7) Kamoun, E. A.; Kenawy, E.-R. S.; Chen, X. A Review on Polymeric Hydrogel Membranes for Wound Dressing Applications: PVA-Based Hydrogel Dressings. *Journal of Advanced Research* **2017**, *8* (3), 217–233. https://doi.org/10.1016/j.jare.2017.01.005.

(8) Yan, G.; Zhang, X.; Li, M.; Zhao, X.; Zeng, X.; Sun, Y.; Tang, X.; Lei, T.; Lin, L. Stability of Soluble Dialdehyde Cellulose and the Formation of Hollow Microspheres: Optimization and Characterization. *ACS Sustainable*

Chem. Eng. **2019**, *7* (2), 2151–2159. https://doi.org/10.1021/acssuschemeng.8b04825.

(9) Koprivica, S.; Siller, M.; Hosoya, T.; Roggenstein, W.; Rosenau, T.; Potthast, A. Regeneration of Aqueous Periodate Solutions by Ozone Treatment: A Sustainable Approach for Dialdehyde Cellulose Production. *ChemSusChem* **2016**, *9* (8), 825–833. https://doi.org/10.1002/cssc.201501639.

(10) Ding, W.; Wu, Y. Sustainable Dialdehyde Polysaccharides as Versatile Building Blocks for Fabricating Functional Materials: An Overview. *Carbohydrate Polymers* **2020**, *248*, 116801. https://doi.org/10.1016/j.carbpol.2020.116801.

(11) Dai, W. S.; Barbari, T. A. Hydrogel Membranes with Mesh Size Asymmetry Based on the Gradient Crosslinking of Poly(Vinyl Alcohol). *Journal of Membrane Science* **1999**, *156* (1), 67–79. https://doi.org/10.1016/S0376-7388(98)00330-5.

(12) Peppas, N. A.; Slaughter, B. V.; Kanzelberger, M. A. Hydrogels. In *Polymer Science: A Comprehensive Reference*; Elsevier, 2012; pp 385–395. https://doi.org/10.1016/B978-0-444-53349-4.00226-0.

(13) Sperling, L. H. *Introduction to Physical Polymer Science*, 4th ed.; Wiley: Hoboken, N.J, 2006.

(14) Rosiak, J. M.; Yoshii, F. Hydrogels and Their Medical Applications. *Nuclear Instruments and Methods in Physics Research Section B: Beam Interactions with Materials and Atoms* **1999**, *151* (1–4), 56–64. https://doi.org/10.1016/S0168-583X(99)00118-4.

(15) H. Gulrez, S. K.; Al-Assaf, S.; O, G. Hydrogels: Methods of Preparation, Characterisation and Applications. In *Progress in Molecular and Environmental Bioengineering - From Analysis and Modeling to Technology Applications*; Carpi, A., Ed.; InTech, 2011. https://doi.org/10.5772/24553.

(16) Hennink, W. E.; van Nostrum, C. F. Novel Crosslinking Methods to Design Hydrogels. *Advanced Drug Delivery Reviews* **2002**, *54* (1), 13–36. https://doi.org/10.1016/S0169-409X(01)00240-X.

(17) *Hydrogels: Biological Properties and Applications*; Barbucci, R., Ed.; Springer: Milan ; New York, 2009.

(18) Li, J.; Mooney, D. J. Designing Hydrogels for Controlled Drug Delivery. *Nat Rev Mater* **2016**, *1* (12), 16071. https://doi.org/10.1038/natrevmats.2016.71.

(19) Li, J.; Hu, Y.; Vlassak, J. J.; Suo, Z. Experimental Determination of Equations of State for Ideal Elastomeric Gels. *Soft Matter* **2012**, *8* (31), 8121. https://doi.org/10.1039/c2sm25437a.

(20) Drury, J. L.; Dennis, R. G.; Mooney, D. J. The Tensile Properties of Alginate Hydrogels. *Biomaterials* **2004**, *25* (16), 3187–3199. https://doi.org/10.1016/j.biomaterials.2003.10.002.

(21) Rehmann, M. S.; Skeens, K. M.; Kharkar, P. M.; Ford, E. M.; Maverakis, E.; Lee, K. H.; Kloxin, A. M. Tuning and Predicting Mesh Size and Protein

Release from Step Growth Hydrogels. *Biomacromolecules* **2017**, *18* (10), 3131–3142. https://doi.org/10.1021/acs.biomac.7b00781.

(22) Flory, P. J.; Rehner, J. Statistical Mechanics of Cross-Linked Polymer Networks II. Swelling. *The Journal of Chemical Physics* **1943**, *11* (11), 521–526. https://doi.org/10.1063/1.1723792.

(23) Waters, D. J.; Engberg, K.; Parke-Houben, R.; Hartmann, L.; Ta, C. N.; Toney, M. F.; Frank, C. W. Morphology of Photopolymerized End-Linked Poly(Ethylene Glycol) Hydrogels by Small-Angle X-Ray Scattering. *Macromolecules* **2010**, *43* (16), 6861–6870. https://doi.org/10.1021/ma101070s.

(24) Krogstad, D. V.; Choi, S.-H.; Lynd, N. A.; Audus, D. J.; Perry, S. L.; Gopez, J. D.; Hawker, C. J.; Kramer, E. J.; Tirrell, M. V. Small Angle Neutron Scattering Study of Complex Coacervate Micelles and Hydrogels Formed from Ionic Diblock and Triblock Copolymers. *J. Phys. Chem. B* **2014**, *118* (45), 13011–13018. https://doi.org/10.1021/jp509175a.

(25) Ritger, P. L.; Peppas, N. A. A Simple Equation for Description of Solute Release I. Fickian and Non-Fickian Release from Non-Swellable Devices in the Form of Slabs, Spheres, Cylinders or Discs. *Journal of Controlled Release* **1987**, *5* (1), 23–36. https://doi.org/10.1016/0168-3659(87)90034-4.

(26) Ritger, P. L.; Peppas, N. A. A Simple Equation for Description of Solute Release II. Fickian and Anomalous Release from Swellable Devices. *Journal of Controlled Release* **1987**, *5* (1), 37–42. https://doi.org/10.1016/0168-3659(87)90035-6.

(27) Lin, C.-C.; Metters, A. T. Hydrogels in Controlled Release Formulations: Network Design and Mathematical Modeling. *Advanced Drug Delivery Reviews* **2006**, *58* (12–13), 1379–1408. https://doi.org/10.1016/j.addr.2006.09.004.

(28) Jin, M.; Shi, J.; Zhu, W.; Yao, H.; Wang, D.-A. Polysaccharide-Based Biomaterials in Tissue Engineering: A Review. *Tissue Engineering Part B: Reviews* **2021**, *27* (6), 604–626. https://doi.org/10.1089/ten.teb.2020.0208.

(29) Kristiansen, K. A.; Potthast, A.; Christensen, B. E. Periodate Oxidation of Polysaccharides for Modification of Chemical and Physical Properties. *Carbohydrate Research* **2010**, *345* (10), 1264–1271. https://doi.org/10.1016/j.carres.2010.02.011.

(30) Kim, U.-J.; Kuga, S.; Wada, M.; Okano, T.; Kondo, T. Periodate Oxidation of Crystalline Cellulose. *Biomacromolecules* **2000**, *1* (3), 488–492. https://doi.org/10.1021/bm0000337.

(31) Muchová, M.; Münster, L.; Vávrová, A.; Capáková, Z.; Kuřitka, I.; Vícha, J. Comparison of Dialdehyde Polysaccharides as Crosslinkers for Hydrogels: The Case of Poly(Vinyl Alcohol). *Carbohydrate Polymers* **2022**, *279*, 119022. https://doi.org/10.1016/j.carbpol.2021.119022.

(32) Sarwat, F.; Qader, S. A. U.; Aman, A.; Ahmed, N. Production & Characterization of a Unique Dextran from an Indigenous *Leuconostoc*

Mesenteroides CMG713. *Int. J. Biol. Sci.* **2008**, 379–386. https://doi.org/10.7150/ijbs.4.379.

(33) Maia, J.; Carvalho, R. A.; Coelho, J. F. J.; Simões, P. N.; Gil, M. H. Insight on the Periodate Oxidation of Dextran and Its Structural Vicissitudes. *Polymer* **2011**, *52* (2), 258–265. https://doi.org/10.1016/j.polymer.2010.11.058.

(34) Münster, L.; Fojtů, M.; Capáková, Z.; Muchová, M.; Musilová, L.; Vaculovič, T.; Balvan, J.; Kuřitka, I.; Masařík, M.; Vícha, J. Oxidized Polysaccharides for Anticancer-Drug Delivery: What Is the Role of Structure? *Carbohydrate Polymers* **2021**, *257*, 117562. https://doi.org/10.1016/j.carbpol.2020.117562.

(35) Fraser, J. R. E.; Laurent, T. C.; Laurent, U. B. G. Hyaluronan: Its Nature, Distribution, Functions and Turnover. *Journal of Internal Medicine* **1997**, *242* (1), 27–33. https://doi.org/10.1046/j.1365-2796.1997.00170.x.

(36) Fallacara, A.; Baldini, E.; Manfredini, S.; Vertuani, S. Hyaluronic Acid in the Third Millennium. *Polymers* **2018**, *10* (7), 701. https://doi.org/10.3390/polym10070701.

(37) Boeden, H.-F.; Pommerening, K.; Becker, M.; Rupprich, C.; Holtzhauer, M.; Loth, F.; Müller, R.; Bertram, D. Bead Cellulose Derivatives as Supports for Immobilization and Chromatographic Purification of Proteins. *Journal of Chromatography A* **1991**, *552*, 389–414. https://doi.org/10.1016/S0021-9673(01)95956-4.

(38) Maekawa, E.; Koshijima, T. Properties of 2,3-Dicarboxy Cellulose Combined with Various Metallic Ions. *J. Appl. Polym. Sci.* **1984**, *29* (7), 2289–2297. https://doi.org/10.1002/app.1984.070290705.

(39) Gurvich, A. E.; Lechtzind, E. V. High Capacity Immunoadsorbents Based on Preparations of Reprecipitated Cellulose. *Molecular Immunology* **1982**, *19* (4), 637–640. https://doi.org/10.1016/0161-5890(82)90233-4.

(40) Wolf, B.; Finke, I. [The use of bead cellulose for controlled drug liberation. 5. Binding of benzocaine as a model drug to dialdehyde-bead cellulose and its in vitro liberation]. *Pharmazie* **1992**, *47* (2), 121–125.

(41) Li, J.; Wan, Y.; Li, L.; Liang, H.; Wang, J. Preparation and Characterization of 2,3-Dialdehyde Bacterial Cellulose for Potential Biodegradable Tissue Engineering Scaffolds. *Materials Science and Engineering: C* **2009**, *29* (5), 1635–1642. https://doi.org/10.1016/j.msec.2009.01.006.

(42) Patterson, J.; Siew, R.; Herring, S. W.; Lin, A. S. P.; Guldberg, R.; Stayton, P. S. Hyaluronic Acid Hydrogels with Controlled Degradation Properties for Oriented Bone Regeneration. *Biomaterials* **2010**, *31* (26), 6772–6781. https://doi.org/10.1016/j.biomaterials.2010.05.047.

(43) Li, S.; Pei, M.; Wan, T.; Yang, H.; Gu, S.; Tao, Y.; Liu, X.; Zhou, Y.; Xu, W.; Xiao, P. Self-Healing Hyaluronic Acid Hydrogels Based on Dynamic Schiff Base Linkages as Biomaterials. *Carbohydrate Polymers* **2020**, *250*, 116922. https://doi.org/10.1016/j.carbpol.2020.116922.

(44) Fu, Y.; Zhang, J.; Wang, Y.; Li, J.; Bao, J.; Xu, X.; Zhang, C.; Li, Y.; Wu, H.; Gu, Z. Reduced Polydopamine Nanoparticles Incorporated Oxidized Dextran/Chitosan Hybrid Hydrogels with Enhanced Antioxidative and Antibacterial Properties for Accelerated Wound Healing. *Carbohydrate Polymers* **2021**, *257*, 117598. https://doi.org/10.1016/j.carbpol.2020.117598.

(45) Babjaková, E.; Branná, P.; Kuczyńska, M.; Rouchal, M.; Prucková, Z.; Dastychová, L.; Vícha, J.; Vícha, R. An Adamantane-Based Disubstituted Binding Motif with Picomolar Dissociation Constants for Cucurbit[n]Urils in Water and Related Quaternary Assemblies. *RSC Adv.* **2016**, *6* (107), 105146–105153. https://doi.org/10.1039/C6RA23524G.

(46) Concheiro, A.; Alvarez-Lorenzo, C. Chemically Cross-Linked and Grafted Cyclodextrin Hydrogels: From Nanostructures to Drug-Eluting Medical Devices. *Advanced Drug Delivery Reviews* **2013**, *65* (9), 1188–1203. https://doi.org/10.1016/j.addr.2013.04.015.

(47) Vatanpour, V.; Teber, O. O.; Mehrabi, M.; Koyuncu, I. Polyvinyl Alcohol-Based Separation Membranes: A Comprehensive Review on Fabrication Techniques, Applications and Future Prospective. *Materials Today Chemistry* **2023**, *28*, 101381. https://doi.org/10.1016/j.mtchem.2023.101381.

(48) Kumar, A.; Han, S. S. PVA-Based Hydrogels for Tissue Engineering: A Review. *International Journal of Polymeric Materials and Polymeric Biomaterials* **2017**, *66* (4), 159–182. https://doi.org/10.1080/00914037.2016.1190930.

(49) Kamoun, E. A.; Chen, X.; Mohy Eldin, M. S.; Kenawy, E.-R. S. Crosslinked Poly(Vinyl Alcohol) Hydrogels for Wound Dressing Applications: A Review of Remarkably Blended Polymers. *Arabian Journal of Chemistry* **2015**, *8* (1), 1–14. https://doi.org/10.1016/j.arabjc.2014.07.005.

(50) Asy-Syifa, N.; Kusjuriansah; Waresindo, W. X.; Edikresnha, D.; Suciati, T.; Khairurrijal, K. The Study of the Swelling Degree of the PVA Hydrogel with Varying Concentrations of PVA. *J. Phys.: Conf. Ser.* **2022**, *2243* (1), 012053. https://doi.org/10.1088/1742-6596/2243/1/012053.

(51) Chen, Y.; Li, J.; Lu, J.; Ding, M.; Chen, Y. Synthesis and Properties of Poly(Vinyl Alcohol) Hydrogels with High Strength and Toughness. *Polymer Testing* **2022**, *108*, 107516. https://doi.org/10.1016/j.polymertesting.2022.107516.

(52) Rodríguez-Rodríguez, R.; Espinosa-Andrews, H.; Velasquillo-Martínez, C.; García-Carvajal, Z. Y. Composite Hydrogels Based on Gelatin, Chitosan and Polyvinyl Alcohol to Biomedical Applications: A Review. *International Journal of Polymeric Materials and Polymeric Biomaterials* **2020**, *69* (1), 1–20. https://doi.org/10.1080/00914037.2019.1581780.

(53) Wang, M.; Bai, J.; Shao, K.; Tang, W.; Zhao, X.; Lin, D.; Huang, S.; Chen, C.; Ding, Z.; Ye, J. Poly(Vinyl Alcohol) Hydrogels: The Old and New Functional Materials. *International Journal of Polymer Science* **2021**, *2021*, 1–16. https://doi.org/10.1155/2021/2225426.

(54) Münster, L.; Vícha, J.; Klofáč, J.; Masař, M.; Hurajová, A.; Kuřitka, I. Dialdehyde Cellulose Crosslinked Poly(Vinyl Alcohol) Hydrogels: Influence of Catalyst and Crosslinker Shelf Life. *Carbohydrate Polymers* **2018**, *198*, 181–190. https://doi.org/10.1016/j.carbpol.2018.06.035.

(55) Bolto, B.; Tran, T.; Hoang, M.; Xie, Z. Crosslinked Poly(Vinyl Alcohol) Membranes. *Progress in Polymer Science* **2009**, *34* (9), 969–981. https://doi.org/10.1016/j.progpolymsci.2009.05.003.

(56) Miyazaki, T.; Takeda, Y.; Akane, S.; Itou, T.; Hoshiko, A.; En, K. Role of Boric Acid for a Poly (Vinyl Alcohol) Film as a Cross-Linking Agent: Melting Behaviors of the Films with Boric Acid. *Polymer* **2010**, *51* (23), 5539–5549. https://doi.org/10.1016/j.polymer.2010.09.048.

(57) Putro, P. A.; Sulaeman, A. S.; Maddu, A. Polyvinyl Alcohol-Based Hydrogel: A Systematic Literature Review on Thermal Properties by Differential Scanning Calorimetry. *J. Phys.: Conf. Ser.* **2021**, *2019* (1), 012101. https://doi.org/10.1088/1742-6596/2019/1/012101.

(58) Chu, L.; Liu, C.; Zhou, G.; Xu, R.; Tang, Y.; Zeng, Z.; Luo, S. A Double Network Gel as Low Cost and Easy Recycle Adsorbent: Highly Efficient Removal of Cd(II) and Pb(II) Pollutants from Wastewater. *Journal of Hazardous Materials* **2015**, *300*, 153–160. https://doi.org/10.1016/j.jhazmat.2015.06.070.

(59) Guo, Y.; Lu, H.; Zhao, F.; Zhou, X.; Shi, W.; Yu, G. Biomass-Derived Hybrid Hydrogel Evaporators for Cost-Effective Solar Water Purification. *Adv. Mater.* **2020**, *32* (11), 1907061. https://doi.org/10.1002/adma.201907061.

(60) Zhao, F.; Zhou, X.; Shi, Y.; Qian, X.; Alexander, M.; Zhao, X.; Mendez, S.; Yang, R.; Qu, L.; Yu, G. Highly Efficient Solar Vapour Generation via Hierarchically Nanostructured Gels. *Nature Nanotech* **2018**, *13* (6), 489–495. https://doi.org/10.1038/s41565-018-0097-z.

(61) Baker, M. I.; Walsh, S. P.; Schwartz, Z.; Boyan, B. D. A Review of Polyvinyl Alcohol and Its Uses in Cartilage and Orthopedic Applications. *J. Biomed. Mater. Res.* **2012**, *100B* (5), 1451–1457. https://doi.org/10.1002/jbm.b.32694.

(62) Cavalieri, F.; Chiessi, E.; Villa, R.; Viganò, L.; Zaffaroni, N.; Telling, M. F.; Paradossi, G. Novel PVA-Based Hydrogel Microparticles for Doxorubicin Delivery. *Biomacromolecules* **2008**, *9* (7), 1967–1973. https://doi.org/10.1021/bm800225v.

(63) Ruiz, J.; Mantecón, A.; Cádiz, V. Investigation of Loading and Release in PVA-Based Hydrogels: Loading and Release in PVA-Based Hydrogels. *J. Appl. Polym. Sci.* **2002**, *85* (8), 1644–1651. https://doi.org/10.1002/app.10696.

(64) Chen, Y.; Song, J.; Wang, S.; Liu, W. PVA-Based Hydrogels: Promising Candidates for Articular Cartilage Repair. *Macromol. Biosci.* **2021**, *21* (10), 2100147. https://doi.org/10.1002/mabi.202100147.

(65) Husain, M. S. B.; Gupta, A.; Alashwal, B. Y.; Sharma, S. Synthesis of PVA/PVP Based Hydrogel for Biomedical Applications: A Review. *Energy Sources, Part A: Recovery, Utilization, and Environmental Effects* **2018**, *40* (20), 2388–2393. https://doi.org/10.1080/15567036.2018.1495786.

(66) Muchová, M.; Münster, L.; Capáková, Z.; Mikulcová, V.; Kuřitka, I.; Vícha, J. Design of Dialdehyde Cellulose Crosslinked Poly(Vinyl Alcohol) Hydrogels for Transdermal Drug Delivery and Wound Dressings. *Materials Science and Engineering: C* **2020**, *116*, 111242. https://doi.org/10.1016/j.msec.2020.111242.

(67) Münster, L.; Capáková, Z.; Fišera, M.; Kuřitka, I.; Vícha, J. Biocompatible Dialdehyde Cellulose/Poly(Vinyl Alcohol) Hydrogels with Tunable Properties. *Carbohydrate Polymers* **2019**, *218*, 333–342. https://doi.org/10.1016/j.carbpol.2019.04.091.

(68) Münster, L.; Vícha, J.; Klofáč, J.; Masař, M.; Kucharczyk, P.; Kuřitka, I. Stability and Aging of Solubilized Dialdehyde Cellulose. *Cellulose* **2017**, *24* (7), 2753–2766. https://doi.org/10.1007/s10570-017-1314-x.

(69) Trauer, S.; Patzelt, A.; Otberg, N.; Knorr, F.; Rozycki, C.; Balizs, G.; Büttemeyer, R.; Linscheid, M.; Liebsch, M.; Lademann, J. Permeation of Topically Applied Caffeine through Human Skin - a Comparison of *in Vivo* and *in Vitro* Data. *British Journal of Clinical Pharmacology* **2009**, *68* (2), 181–186. https://doi.org/10.1111/j.1365-2125.2009.03463.x.

(70) Bonina, F.; Bader, S.; Montenegro, L.; Scrofani, C.; Visca, M. Three Phase Emulsions for Controlled Delivery in the Cosmetic Field. *Int J Cosmet Sci* **1992**, *14* (2), 65–74. https://doi.org/10.1111/j.1467-2494.1992.tb00040.x.

(71) Santander-Ortega, M. J.; Stauner, T.; Loretz, B.; Ortega-Vinuesa, J. L.; Bastos-González, D.; Wenz, G.; Schaefer, U. F.; Lehr, C. M. Nanoparticles Made from Novel Starch Derivatives for Transdermal Drug Delivery. *Journal of Controlled Release* **2010**, *141* (1), 85–92. https://doi.org/10.1016/j.jconrel.2009.08.012.

(72) Pilloni, M.; Ennas, G.; Casu, M.; Fadda, A. M.; Frongia, F.; Marongiu, F.; Sanna, R.; Scano, A.; Valenti, D.; Sinico, C. Drug Silica Nanocomposite: Preparation, Characterization and Skin Permeation Studies. *Pharmaceutical Development and Technology* **2013**, *18* (3), 626–633. https://doi.org/10.3109/10837450.2011.653821.

(73) Veelaert, S.; de Wit, D.; Gotlieb, K. F.; Verhé, R. Chemical and Physical Transitions of Periodate Oxidized Potato Starch in Water. *Carbohydrate Polymers* **1997**, *33* (2–3), 153–162. https://doi.org/10.1016/S0144-8617(97)00046-5.

LIST OF FIGURES

LIST OF TABLES

LIST OF ABBREVIATIONS AND SYMBOLS
ABBREVIATIONS

DXA	2,3 dialdehyde dextran	PVA	poly(vinyl alcohol)
DAC	2,3-dialdehyde cellulose	SEM	scanning electron microscopy
DXI	2,3-dialdehyde dextrin	d_h	The hydrodynamic radii
DAH	2,3-dialdehyde hyaluronate	Z	zeta potentials
BET	Brunauer-Emmet Teller	M_w	molecular weight
DO	degree of oxidation	PDI	polydispersity index
DH	degrees of hydrolysis	DP	degrees of polymerization
DAPs	dialdehyde polysaccharides	M_n	Number average molecular weight
DLS	dynamic light scattering	M_c	The average molecular weight between crosslinks
FT-IR	Fourier-transform infrared spectroscopy	ξ	network mesh size
GPC	Gel Permeation Chromatography	ρ_c	the crosslink density
GA	glutaraldehyde		

LIST OF PUBLICATIONS

Articles published in journals indexed on Web of Science:

Muchová, M.; Münster, L.; Vávrová, A.; Capáková, Z.; Kuřitka, I.; Vícha, J. Comparison of Dialdehyde Polysaccharides as Crosslinkers for Hydrogels: The Case of Poly(Vinyl Alcohol). *Carbohydrate Polymers* **2022**, *279*, 119022. https://doi.org/10.1016/j.carbpol.2021.119022.

Münster, L.; Fojtů, M.; Capáková, Z.; **Muchová, M.**; Musilová, L.; Vaculovič, T.; Balvan, J.; Kuřitka, I.; Masařík, M.; Vícha, J. Oxidized Polysaccharides for Anticancer-Drug Delivery: What Is the Role of Structure? *Carbohydrate Polymers* **2021**, *257*, 117562. https://doi.org/10.1016/j.carbpol.2020.117562.

Münster, L.; Fojtů, M.; **Muchová, M.**; Latečka, F.; Káčerová, S.; Capáková, Z.; Juriňáková, T.; Kuřitka, I.; Masařík, M.; Vícha, J. Enhancing Cisplatin Anticancer Effectivity and Migrastatic Potential by Modulation of Molecular Weight of Oxidized Dextran Carrier. *Carbohydrate Polymers* **2021**, *272*, 118461. https://doi.org/10.1016/j.carbpol.2021.118461.

Muchová, M.; Münster, L.; Capáková, Z.; Mikulcová, V.; Kuřitka, I.; Vícha, J. Design of Dialdehyde Cellulose Crosslinked Poly(Vinyl Alcohol) Hydrogels for Transdermal Drug Delivery and Wound Dressings. *Materials Science and Engineering: C* **2020**, *116*, 111242. https://doi.org/10.1016/j.msec.2020.111242.

Důbravová, A.; **Muchová, M**.; Škoda, D.; Lovecká, L.; Šimoníková, L.; Kuřitka, I.; Vícha, J.; Münster, L. Highly Efficient Affinity Anchoring of Gold Nanoparticles on Chitosan Nanofibers via Dialdehyde Cellulose for Reusable Catalytic Devices. *Carbohydrate Polymers* **2024**, *323*, 121435. https://doi.org/10.1016/j.carbpol.2023.121435.

Manuscript under revision in international journals with an impact factor:

Káčerová S., Muchová M., Doudová H., Münster L., Hanulíková B., Víchová Z.,Valášková K., Kašpárková V., Kuřitka I., Humpolíček P., Vašíček O., Vícha J. Antibacterial, anti-oxidant, conductive, and anti-inflammatory polypyrrole/chitosan/dialdehyde cellulose hydrogel wound dressings

Conferences:

International conference - Active participation: **Monika Muchová** , Důbravová Alžběta, Lovecká Lenka, Kuřitka Ivo, Vícha Jan, Münster Lukáš. Pilot Preparation Study of Gold Nanoparticle-Chitosan Composite Catalyst. NANOCON (18-20 October 2023), Brno.

International conference: Káčerová Simona, Vícha Jan, Víchová Zdenka, **Muchová Monika**, Münster Lukáš, Vašíček Ondřej, Humpolíček Petr. Bioactive Films Based on Chitosan and Polypyrrole. ECIS 2022: 36th European Colloid & Interface Society Conference 4-9 September 2022 Chania, Crete, Greece, 2022

Proofs of concept:

Gold nanoparticles prepared using selectively oxidized polysaccharide. Vávrová Alžběta; Kuřitka Ivo; Vícha Jan; Münster Lukáš; **Muchová Monika**.

Antibacterial photocatalytic composites based on acetylated chitosans doped by ZnO. Münster Lukáš; Kuřitka Ivo; Vícha Jan; Masař Milan; **Muchová Monika**.

CURRICULUM VITAE

Personal information	
Name	Monika Muchová
Address	Třída Obránců Mírů 2, Bruntál 792 01
E-mail	m_muchova@utb.cz
Nationality	Czech
Date of birth	01.08.1995
Education	**2019-2024** – *Doctoral degree student* *Technology of macromolecular compounds*, Tomas Bata University in Zlín. **2017-2019** – *Mater´s degree* *Food Chemistry and Technology*, Tomas Bata University in Zlín. **2014-2017** – *Bachelor´s degree* *Food Chemistry and Technology*, Tomas Bata University in Zlín.
Education stays	**September-November 2022** University of Aveiro, traineeship – Immobilization of oxidative enzymes on nanofibers,Universidade de Aveiro, 3810-193 Aveiro, Portugal
Work on projects	**IGA/CPS/2023/006** "Preparation and characterization of advanced functional nanocomposite systems" **OP PIK CZ.01.1.02/0.0/0.0/20_321/0025211**- Research and development of a new generation of anti-corrosion pigments that multiply the protection of metal surfaces with an emphasis on their ecological and rational economic efficiency (2022-2023) **GAČR 23-07361S** Synthesis of gold nanoparticles for SERS and catalysis guided by selectively oxidized polysaccharides **IGA/CPS/2022/002** "Preparation and characterization of advanced nanocomposite systems" **IGA/CPS/2021/002** "Preparation and characterization of nanocomposite systems", principal investigator **IGA/CPS/2020/003** "Preparation and characterization of nanoparticles for advanced applications"
Pedagogic activities	Participation on teaching in laboratory classes of "The Basics of Food Packaging", TCPM/TP5ZB (FT, UTB).

Preparation of (bio)polymer matrices for substance transfer and study of their release

Příprava (bio)polymerních matric pro přenos látek a studium jejich uvolňování

Doctoral Thesis Summary